



HAL
open science

New MraYAA Inhibitors with an Aminoribosyl Uridine Structure and an Oxadiazole

Hongwei Wan, Raja Ben Othman, Laurent Le Corre, Mélanie Poinot, Martin Oliver, Ana Amoroso, Bernard Joris, Thierry Touzé, Rodolphe Auger, Sandrine Calvet-Vitale, et al.

► **To cite this version:**

Hongwei Wan, Raja Ben Othman, Laurent Le Corre, Mélanie Poinot, Martin Oliver, et al.. New MraYAA Inhibitors with an Aminoribosyl Uridine Structure and an Oxadiazole. *Antibiotics*, 2022, 11 (9), pp.1189. 10.3390/antibiotics11091189. hal-03805942

HAL Id: hal-03805942

<https://hal.science/hal-03805942v1>


Submitted on 17 Nov 2022

HAL is a multi-disciplinary open access archive for the deposit and dissemination of scientific research documents, whether they are published or not. The documents may come from teaching and research institutions in France or abroad, or from public or private research centers.

L'archive ouverte pluridisciplinaire **HAL**, est destinée au dépôt et à la diffusion de documents scientifiques de niveau recherche, publiés ou non, émanant des établissements d'enseignement et de recherche français ou étrangers, des laboratoires publics ou privés.

Article

New $MraY_{AA}$ Inhibitors with an Aminoribosyl Uridine Structure and an Oxadiazole

Hongwei Wan ¹, Raja Ben Othman ¹, Laurent Le Corre ¹ , Mélanie Poinso ¹, Martin Oliver ¹ , Ana Amoroso ² , Bernard Joris ², Thierry Touzé ³, Rodolphe Auger ³, Sandrine Calvet-Vitale ¹ , Michaël Bosco ^{1,*}  and Christine Gravier-Pelletier ^{1,*} 

¹ Université Paris Cité, CNRS, Laboratoire de Chimie et de Biochimie Pharmacologiques et Toxicologiques, F-75006 Paris, France

² Unité de Physiologie et Génétique Bactériennes, Centre d'Ingénierie des Protéines, Département des Sciences de la Vie, Université de Liège, Sart Tilman, B4000 Liège, Belgium

³ Institute for Integrative Biology of the Cell (I2BC), CNRS, Université Paris Sud, CEA, F-91405 Orsay, France

* Correspondence: michael.bosco@u-paris.fr (M.B.); christine.gravier-pelletier@u-paris.fr (C.G.-P.); Tel.: +33-176-534 246 (M.B.); +33-176-534-228 (C.G.-P.)

Abstract: New inhibitors of the bacterial transferase $MraY$ from *Aquifex aeolicus* ($MraY_{AA}$), based on the aminoribosyl uridine central core of known natural $MraY$ inhibitors, have been designed to generate interaction of their oxadiazole linker with the key amino acids (H324 or H325) of the enzyme active site, as observed for the highly potent inhibitors carbacaprazamycin, muraymycin D2 and tunicamycin. A panel of ten compounds was synthesized notably thanks to a robust microwave-activated one-step sequence for the synthesis of the oxadiazole ring that involved the *O*-acylation of an amidoxime and subsequent cyclization. The synthesized compounds, with various hydrophobic substituents on the oxadiazole ring, were tested against the $MraY_{AA}$ transferase activity. Although with poor antibacterial activity, nine out of the ten compounds revealed the inhibition of the $MraY_{AA}$ activity in the range of 0.8 μ M to 27.5 μ M.

Keywords: $MraY$ transferase; inhibitors synthesis; muraymycin analogs; molecular modeling; inhibition tests



Citation: Wan, H.; Ben Othman, R.; Le Corre, L.; Poinso, M.; Oliver, M.; Amoroso, A.; Joris, B.; Touzé, T.; Auger, R.; Calvet-Vitale, S.; et al. New $MraY_{AA}$ Inhibitors with an Aminoribosyl Uridine Structure and an Oxadiazole. *Antibiotics* **2022**, *11*, 1189. <https://doi.org/10.3390/antibiotics11091189>

Academic Editors: Marc Maresca, Martina Hrast and Carlos M. Franco

Received: 11 July 2022

Accepted: 30 August 2022

Published: 2 September 2022

Publisher's Note: MDPI stays neutral with regard to jurisdictional claims in published maps and institutional affiliations.



Copyright: © 2022 by the authors. Licensee MDPI, Basel, Switzerland. This article is an open access article distributed under the terms and conditions of the Creative Commons Attribution (CC BY) license (<https://creativecommons.org/licenses/by/4.0/>).

1. Introduction

Infectious diseases are one of the most important causes of human death, and bacterial antimicrobial resistance (AMR) is a major threat for human health [1–3]. Based on predictive statistical models, 4.95 million deaths are estimated to be associated with bacterial AMR in 2019, including 1.27 million deaths attributable to bacterial AMR [4]. In addition to its impact on human health [5], antibiotic resistance also has a significant economic cost, notably on the increase in hospital costs due to nosocomial infections [6–9]. One way to fight bacterial AMR is to focus on biological targets displaying a new mode of action compared to those of the approved antibiotics. Considering their high specificity and their unique occurrence in bacteria, enzymes involved in peptidoglycan biosynthesis [10,11] are promising targets, since each of them is essential for the bacterial growth. In this context, our goal is to focus on the inhibition of the $MraY$ transferase [12], which is an unexploited target. Indeed, even if the discovery of potent $MraY$ inhibitors is the subject of intense research efforts, none of the resulting compounds are being investigated in clinical trials. This represents a major advantage that can delay the emergence of drug resistance. This integral membrane protein, essential to bacterial growth and ubiquitous in the bacterial world [13–15], catalyzes the first membrane-associated step of peptidoglycan biosynthesis: the transfer of UDP-MurNAc-pentapeptide on undecaprenylphosphate ($C_{55}P$) to form the lipid I.

Several families of natural $MraY$ inhibitors are known, notably the widely represented one of peptidonucleosidic antibiotics, such as liposidomycins [16–18], muraymycins [19]

and caprazamycins [20,21]. All of these compounds share a common aminoribosyl uridine scaffold that has been shown to be important for their biological activity [22–24]. The synthesis of the simplified analogs of these complex natural compounds [25–28] retaining antibacterial activity is a challenge, and significant progress towards this goal has been made [29–36]. The crystallographic structure of *MraY* from *Aquifex aeolicus* (*MraY_{AA}*) in complex with several ligands has been solved (muraymycin D2 (*MurD2*, PDB: 5CKR) [37] and carbacaprazamycin (PDB: 6OYH) [38]), permitting the S. Y. Lee group to define several hot spots (HS) of the privileged interaction of the co-crystallized inhibitors with the *MraY* active site [38]. We also developed the synthesis of several series of inhibitors based on this aminoribosyl uridine core, the chemical diversity being introduced on the scaffold through various linkers, either cyclic such as C- and N-triazoles [39,40], or acyclic, such as urea [41], amide, sulfonamide, squaramide or diamide [42]. The docking of the triazole-containing inhibitors, in either the 5CKR [30] or 6OYH [31] structural models of *MraY_{AA}*, revealed no significant interactions of the triazole with the amino acids of the active site (Figure 1, 1A). In the present work, considering this lack of stabilizing interaction, we decided to enlarge the panel of inhibitors with a cyclic linker. We focused on oxadiazole-containing ones because the docking of a representative of the targeted oxadiazole series, with a C₁₀ chain as a hydrophobic substituent, showed the interaction of the oxadiazole ring with the key amino acids (H325) of the enzyme active site (Figure 1, 1B), as observed for the highly potent inhibitors carbacaprazamycin, muraymycin D2 and tunicamycin. We hypothesized that this interaction could contribute to generate more active compounds. Furthermore, a panel of hydrophobic substituents with various chain length was selected to study their influence in promoting antibacterial activity.

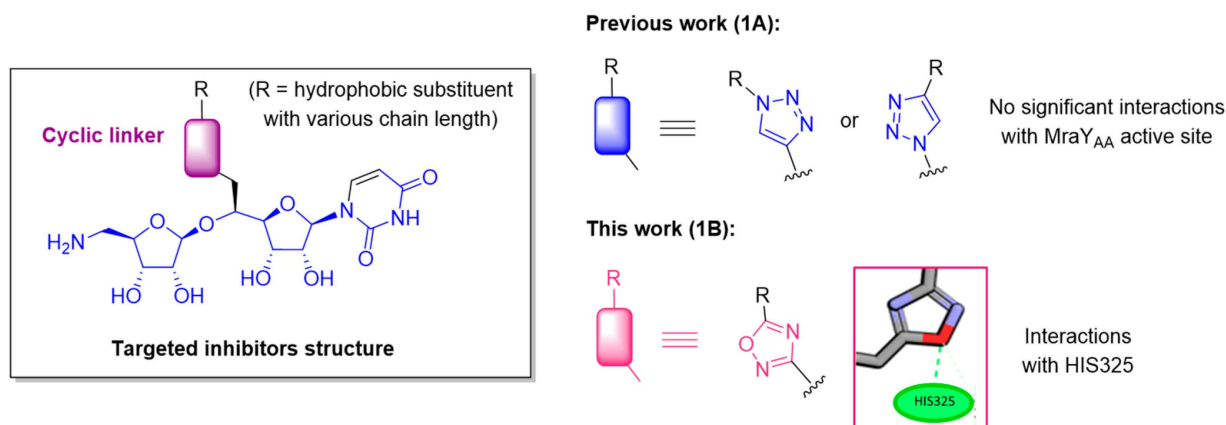


Figure 1. 1A. Structure of the aminoribosyl-uridine-containing *MraY* inhibitors previously synthesized. 1B. Structure of targeted new *MraY* inhibitors.

2. Results and Discussion

2.1. Chemistry

The retrosynthetic analysis towards the targeted compounds is outlined in Figure 2. It would rely on the tandem *O*-acylation-cyclization of the amidoxime **A** with various acyl chlorides **B**, either commercially available or synthesized. The amidoxime **A** could be obtained by a reaction of hydroxylamine with the nitrile **C** resulting from a diastereoselective glycosylation between the nitrile alcohol **E** and a ribosyl donor **D**, activated as a fluoride in its anomeric position and bearing an azido group as a masked amine at C-5. Alcohol **E** should result from the nucleophilic opening of epoxide **F** resulting from uridine.

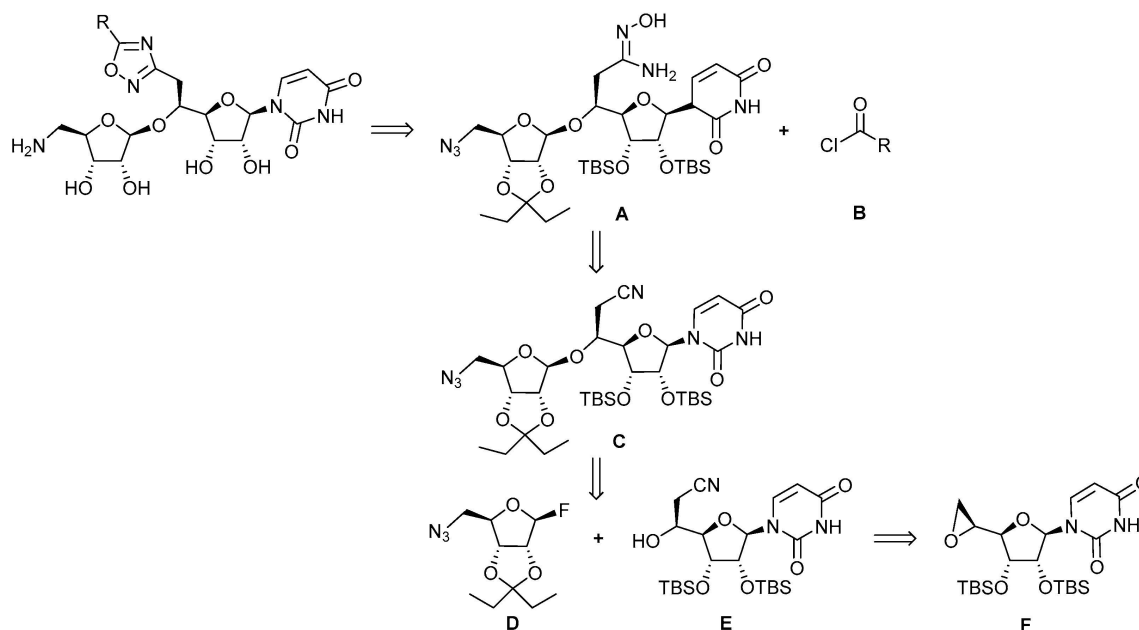
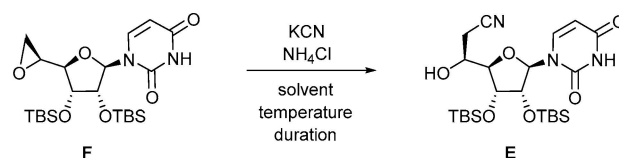


Figure 2. Retrosynthesis of the targeted oxadiazole inhibitors.

The conveniently protected 5-azidoribosyl fluoride **D** was readily synthesized from D-ribose [43]. The synthesis of the cyano alcohol **E** [44] by nucleophilic opening by the potassium cyanide of the epoxide **F** [44] derived from uridine (Scheme 1) has been optimized (Table 1) by screening the number of equivalents of potassium cyanide, the solvent of the reaction, its duration and the eventual addition of ammonium chloride [45].



Scheme 1. Nucleophilic opening of the epoxide **F** by cyanide ions.

Table 1. Optimization of the nucleophilic opening of the epoxide **F** by potassium cyanide.

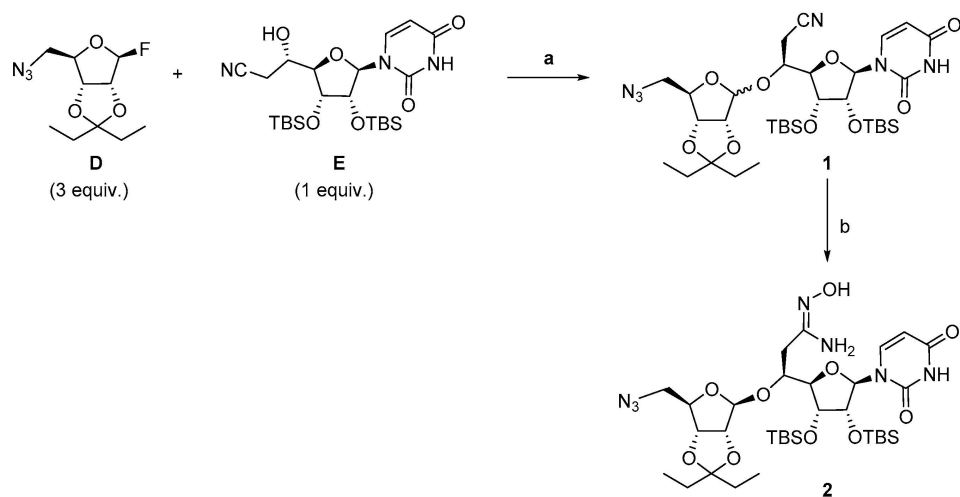
Entry	KCN (equiv.)	Solvent	NH ₄ Cl (equiv.)	T (°C)	Duration	Yield of E (%)
1	8	DMF	1.5	100	16 h	23–68 ^{a,b} or ^c
2	6	DMF	1.5	55	16 h	28 ^b
3	6	CH ₃ CN	1.5	82	16 h	30 ^b
4	6	CH ₃ CN	-	82	16 h	10 ^b
5	6	Toluene	1.5	100	16 h	traces
6	3	Toluene	-	100	16 h	traces
7	6	MeOH/H ₂ O 8/1	1.5	60	2 h	84 ^c
8	3	MeOH/H ₂ O 8/1	1.5	60	16 h	62 ^b
9	5	MeOH/H ₂ O 8/1	2.5	60	16 h	94 ^c

^a Partial deprotection of silyl ethers. ^b Percentage of conversion by NMR. ^c Isolated yield.

The previously described conditions [44,45] involving 8 equiv. of KCN and 1.5 equiv. of NH₄Cl in DMF at 100 °C for 16 h (entry 1) led to variable percentages of the conversion and isolated yield (up to 68%) of compound **E** accompanied by the partial deprotection of

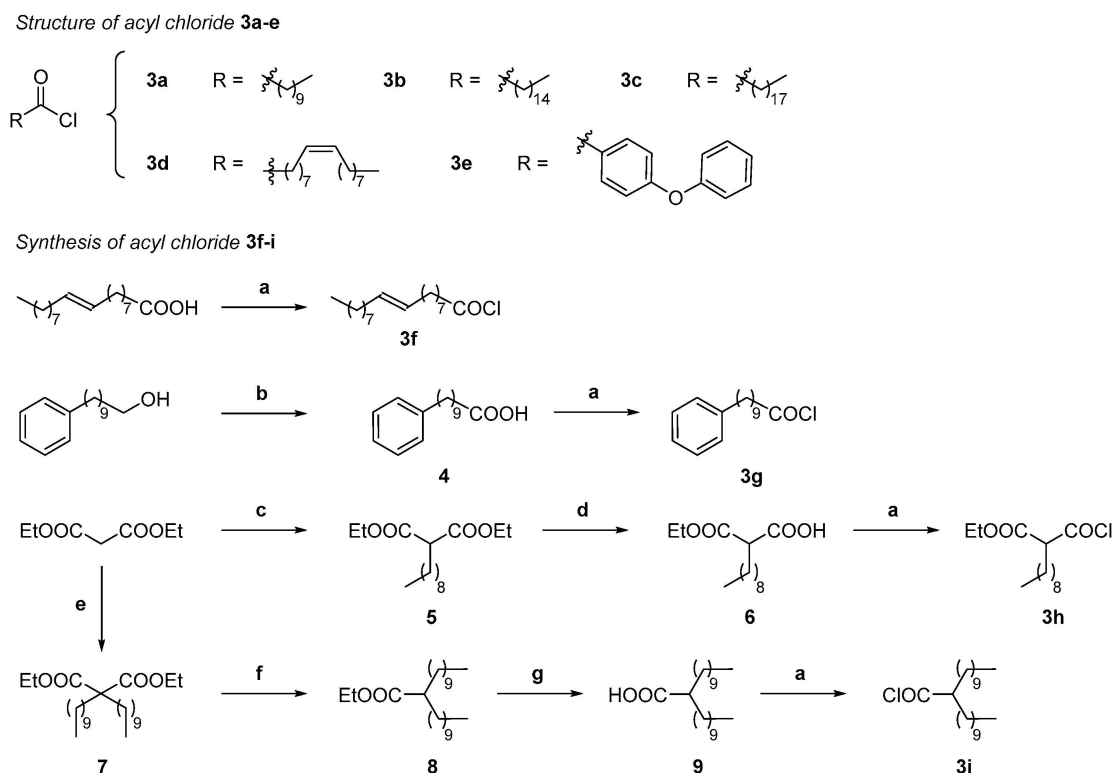
the silyl ethers. Decreasing the amount of KCN to 6 equiv. and the temperature to 55 °C afforded a moderate 28% of the conversion. Replacing the solvent by refluxing CH₃CN with KCN (6 equiv.) in the presence of NH₄Cl (1.5 equiv., entry 3) or in its absence (entry 4) only led to poor conversion and degradation. The reaction was also assayed in toluene at 100 °C with KCN (6 equiv.) and NH₄Cl (1.5 equiv., entry 5) or without NH₄Cl (entry 6) for 16 h. However, only traces of the expected compound **E** were formed, and the reaction mixture turned out to be brownish, characteristic of silyl ethers deprotection. Finally, the reaction was attempted in a MeOH/H₂O 8/1 mixture at 60 °C for 2 h in the presence of KCN (6 equiv.) and NH₄Cl (1.5 equiv., entry 7), leading to an improved 84% isolated yield of compound **E**. Decreasing the amount of KCN (3 equiv.) and increasing the duration of the reaction to 16 h (entry 8) was detrimental to the progress of the reaction, leading to 62% of conversion. The best optimized conditions (entry 9) were revealed to be the use of KCN (5 equiv.) and NH₄Cl (2.5 equiv.) in MeOH/H₂O 8/1 at 60 °C for 16 h, giving cyanoalcohol **E** in a reproducible 94% isolated yield.

We next turned to the diastereoselective glycosylation reaction of the phthalimido-cyano alcohol **E** by the fluororibose derivative **D** as a ribosyl donor (Scheme 2). This reaction was performed according to the conditions we previously described [40]. However, the number of equivalents of the reaction partners has been optimized. The best conditions involved one equivalent of the phthalimido alcohol **E** and three equivalents of fluorinated azido-ribose **D** that were dried by the azeotropic removal of water with toluene. Then, an excess of 4 Å molecular sieves was added after activation by vacuum drying. The products were dissolved in freshly distilled DCM before the addition of boron trifluoride etherate (4.0 equiv.) at −78 °C. After ten minutes at −78 °C, followed by sixteen hours at room temperature, the crude product **1** was isolated as a 8/2 mixture of β/α diastereoisomers. After separation by flash chromatography, the pure β isomer of the glycosylated compound **1** was obtained in 67% yield. This derivative **1** was then engaged in the formation of the amidoxime **2** by reaction with 50% aqueous hydroxylamine in refluxing methanol, leading to the expected amidoxime **2** in 87% yield.



Scheme 2. Synthesis of the amidoxime **2**. Reagents and conditions: (a) 4 Å MS, BF₃·OEt₂ (4.0 equiv.), −78 °C, 10 min then rt, 16 h, 67% of pure β isomer; (b) 50% aqueous NH₂OH, MeOH reflux, 6 h, 87%.

Starting from the amidoxime **2** intermediate, the synthesis of a series of MraY inhibitors with an oxadiazole linker was then undertaken by the *O*-acylation of the amidoxime **2** with a panel of acyl chlorides **3** (Scheme 3), either commercially available, with various alkyl chain lengths, an eventual unsaturation or aromatic moieties (**3a–3e**), or synthesized according to classical routes (**3f–3i**).

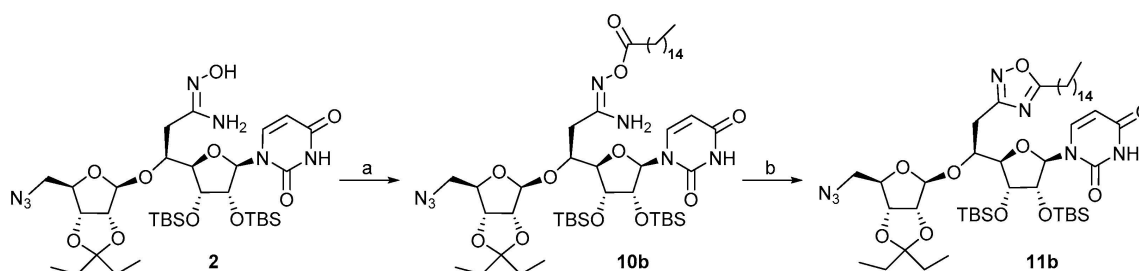


Scheme 3. Structure and/or synthesis of compounds **3a–i**. Reagents and conditions: (a) Oxalyl chloride, dry DMF cat., pentane, r.t., 2 h; (b) CrO_3 , H_2SO_4 , H_2O , acetone, $0\text{ }^\circ\text{C}$ to r.t., 3 h, 80%; (c) $\text{CH}_3(\text{CH}_2)_8\text{I}$ (1 equiv.), K_2CO_3 (5 equiv.), DMF/THF 1/1, overnight, r.t. to $90\text{ }^\circ\text{C}$ to r.t., 91%; (d) (1) KOH (1 equiv.), $\text{EtOH}/\text{H}_2\text{O}$ 10/1, (2) Aqueous HCl , H_2O , 72%; (e) NaH (3 equiv.), $0\text{ }^\circ\text{C}$ 30 min, then $\text{CH}_3(\text{CH}_2)_9\text{I}$ (2.5 equiv.), THF, $0\text{ }^\circ\text{C}$ to r.t., 48 h, 76%; (f) LiCl (2.5 equiv.), H_2O (1.15 equiv.), DMSO, 12 h, r.t., 60%; (g) NaOH , $\text{EtOH}/\text{H}_2\text{O}$ 10/1, overnight (90%).

The choice of the acyl chloride substituents was directed towards long hydrophobic chains (C_{10} – C_{18} , **3a–3c**, **3f**) in aiming at filling the hydrophobic groove HS4 of the MraY active site [38] and at obtaining antibacterial activities, since we previously showed that inhibitors with small chains are probably not sufficient to lead to good antibacterial activities [41]. A diphenyl ether (**3e**) was chosen in agreement with the reported inhibitory activity of MraY [46], and a C_9 -alkyl chain bearing a terminal phenyl group was also selected (**3g**). To potentially fill two hot spots of the active site (HS2 and HS4), disubstituted compounds bearing a C_9 alkyl chain and an ethyl ester (**3h**) and two C_{10} alkyl chains (**3i**) were also targeted. The synthesis of the acyl chlorides **3f–3i** (Scheme 3) was realized by the reaction of the corresponding commercial or synthesized carboxylic acids with oxalyl chloride in the presence of catalytic DMF in pentane [47]. Accordingly, the acyl chloride **3f** bearing a long C_{18} alkyl chain with an *E* unsaturation was performed from the corresponding commercial acid. The 10-phenyl decanoyl chloride **3g** was obtained by the Jones oxidation of the corresponding alcohol into the carboxylic acid **4** that was isolated in 80% yield. The synthesis of the derivative **3h** was carried out by reacting the anion of diethyl malonate generated in the presence of an excess of potassium carbonate in a 1/1 DMF/THF mixture with 1-iododecane, leading to the diester, followed by the selective saponification of the one ester group [48] by potassium hydroxide in a 1/10 $\text{H}_2\text{O}/\text{EtOH}$ mixture, giving the mono acid mono ester **6** in 72% yield. The dialkylated acid **9** resulted from a three-step sequence involving first the dialkylation by 1-iododecane of diethyl malonate in the presence of sodium hydride in THF [49] that was achieved in 78% yield and led to the dialkylated derivative **7**. Then, the decarboethoxylation of this compound **7** in the presence of lithium chloride and H_2O in DMSO [50] afforded the monoethyl ester **8**, which was followed by the saponification of the ester in the presence of sodium hydroxide

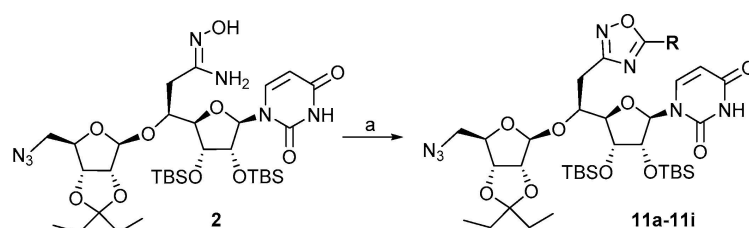
in a 10/1 EtOH/H₂O mixture, giving the dialkylated acid **9**. After treatment of the acids **4**, **6** and **9** with oxalyl chloride as previously mentioned, the resulting crude acyl chlorides **3g–3i** were sufficiently pure to be engaged in the subsequent *O*-acylation step of amidoxime **2** without further purification.

With the amidoxime **2** and acyl chlorides **3a–3i** in hand, we focused on the synthesis of the oxadiazole-containing inhibitors (Scheme 4). The reaction was first attempted in a two-step sequence involving first the *O*-acylation of the amidoxime **2** with palmitoyl chloride **3b** in the presence of DBU in refluxing CH₂Cl₂ leading to compound **10b** in 45% yield, followed by cyclization in toluene under microwave irradiation at 300 W for 3 h at 135 °C. After purification, the oxadiazole **11b** was isolated in 82% yield.



Scheme 4. Synthesis of the oxadiazole **11b**. Reagents and conditions: (a) DBU (2 equiv.), **3b** (2 equiv.), CH₂Cl₂, 0 °C, 15 min, then reflux overnight, 45%; (b) toluene, μ W 300 W, 135 °C, 3 h, 82%.

It has to be mentioned that the cyclization reaction performed in thermic conditions involving 4 days of heating in refluxing toluene only led to traces of the expected compound **11b** and degradation, while part of the starting *O*-acylated amidoxime **10b** was still present. In order to improve the yield and shorten the duration of this two-step sequence, the reaction was then carried out according to a one-pot procedure under microwave irradiation (Scheme 5, Table 2) at 150 °C in toluene in the presence of variable amounts of DBU for different durations.



Scheme 5. Synthesis of the oxadiazoles **11a–11i**. Reagents and conditions: (a) **3a–3i** (1.1 equiv.), DBU (see Table 2) 30 min, r.t. then, μ W 150 °C, toluene.

Table 2. Conditions for the one-pot synthesis of oxadiazole **11b**.

Entry	DBU (equiv.)	t (min)	Yield of 11b ^a (%)
1	2.0	15	28
2	2.5	15	30
3	2.5	30	55

^a Isolated yield.

The reaction was first performed in the presence of DBU (2 equiv.) for 15 min leading to the oxadiazole **11b** in a modest 28% yield (entry 1). Increasing the amount of DBU (2.5 equiv.) slightly improved the yield of the reaction to 30% (entry 2). Finally, the best conditions involved DBU (2.5 equiv.) for 30 min under microwave irradiation at 150 °C in toluene and led to oxadiazole **11b** in 55% yield. Partial degradation was observed with longer reaction time, thus decreasing the yield. These conditions were then applied to the

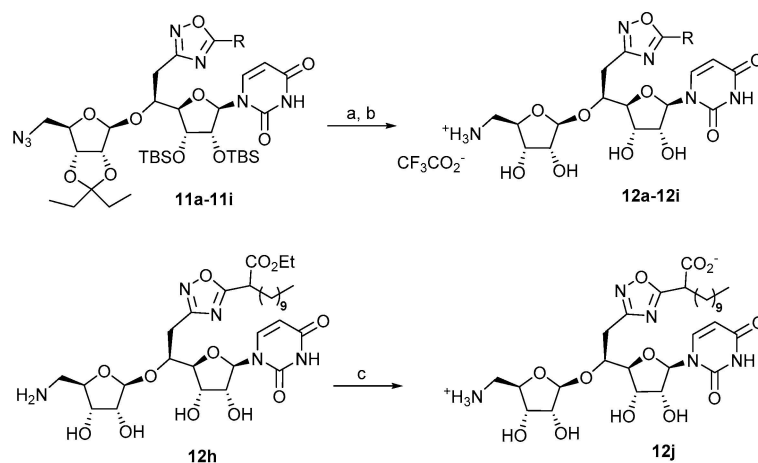
synthesis of the oxadiazoles **11a** and **11c–11i** that were isolated in yields ranging from 42 to 83% (Table 3).

Table 3. Isolated yields for the synthesis of compounds **11a–i** and **12a–i**.

Acyl Chlorides	R	11 Yield ^a (%)	12 Yield ^a (%)
3a	-(CH ₂) ₉ -CH ₃	67	85
3b	-(CH ₂) ₁₄ -CH ₃	55	59
3c	-(CH ₂) ₁₇ -CH ₃	75	40
3d	-(CH ₂) ₇ -CH=CH-(CH ₂) ₇ -CH ₃ (Z)	72	66
3e	-C ₆ H ₄ -O-C ₆ H ₅	42	60
3f	-(CH ₂) ₇ -CH=CH-(CH ₂) ₇ -CH ₃ (E)	83	63
3g	-(CH ₂) ₉ -Ph	58	63
3h	-CH((CH ₂) ₈ -CH ₃)(CO ₂ Et)	58	68
3i	-CH-((CH ₂) ₁₀) ₂	74	22 ^b

^a Isolated yields. ^b Part of the starting compound **11i** was recovered.

The reduction of the azido group of oxadiazoles **11a–11i** was then performed in a 85/15 THF/H₂O mixture under Staudinger conditions using polymer-supported triphenylphosphine to efficiently remove the generated supported triphenylphosphine oxide by filtration. The final acidic hydrolysis of the alcohol protective groups of the resulting crude amines was carried out in a cold 4/1 mixture of trifluoroacetic acid/water. The targeted oxadiazoles inhibitors **12a–12i** were isolated in 22 to 85% overall yield after flash chromatographic purification on silica gel (Scheme 6, Table 3). The saponification of ester **12h** (Scheme 6) was achieved by ammonium hydrogenocarbonate in the presence of triethylamine in methanol leading to the oxadiazole **12j** (Scheme 6).



Scheme 6. Deprotection steps of compounds **11a–11i** and **12h**. Reagents and conditions: (a) PS-PPh₃, THF/H₂O 85/15, r.t., 48 h; (b) TFA/H₂O 4:1, 0 °C, r.t., 16 h; (c) aqueous NH₄HCO₃, Et₃N, MeOH, 17%.

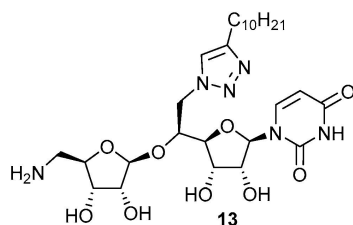
2.2. Biological Studies

The inhibitory activity of the synthesized compounds **12a–12j** was evaluated on Mray transferase purified from *Aquifex aeolicus* (Mray_{AA}) prepared as previously described by Chung et al. [51]. Their activity (Table 4) was compared to the inhibitory activity of the *N*-triazole-containing inhibitor **13** (Figure 3) that we previously synthesized [40] (Table 4). Commercially available tunicamycin from *Streptomyces* sp. was used as a positive control in the test.

Table 4. Inhibitory activity of compounds **12a–12j** against $MraY_{AA}$.

Compound	R	IC ₅₀ (μM) ^{a, b}
Tunicamycin		0.026 ± 0.00
13		1.1 ± 0.0
12a	-(CH ₂) ₉ -CH ₃	0.8 ± 0.1
12b	-(CH ₂) ₁₄ -CH ₃	9.3 ± 0.2
12c	-(CH ₂) ₁₇ -CH ₃	15.8 ± 1.0
12d	-(CH ₂) ₇ -CH=CH-(CH ₂) ₇ -CH ₃ (Z)	18.9 ± 0.9
12e	-C ₆ H ₄ -O-C ₆ H ₅	3.2 ± 0.2
12f	-(CH ₂) ₇ -CH=CH-(CH ₂) ₇ -CH ₃ (E)	17.3 ± 0.3
12g	(CH ₂) ₉ -Ph	5.8 ± 0.1
12h	-CH-((CH ₂) ₈ -CH ₃)-(CO ₂ Et)	27.5 ± 0.7
12i	-CH-((CH ₂) ₁₀) ₂	N.I. ^c
12j	-CH-((CH ₂) ₈ -CH ₃)-(CO ₂ ⁻)	2.9 ± 0.6

^a Experiments were performed in triplicate, and each experiment was repeated at least twice, except for tunicamycin as a control, which was tested twice. ^b All compounds were tested at a final concentration of 10% DMSO to ensure complete solubility. ^c N.I.: No inhibition.

**Figure 3.** Structure of the reference *N*-triazole inhibitor **13**.

As shown in Table 4, nine oxadiazole-containing compounds out of the ten tested are relevant inhibitors of the enzymatic activity of the transferase $MraY_{AA}$ with IC₅₀ ranging from 0.8 μM to 27.5 μM, the best $MraY_{AA}$ inhibitory activity being obtained with a saturated C₁₀ alkyl substituent on the oxadiazole moiety (**12a**). The inhibitory activity of this compound **12a** (0.8 μM) is a bit improved compared to that of the reference *N*-triazole **13** (1.1 μM). Among the compounds with one alkyl chain (**12a**, **12b**, **12c**), the results show that increasing the alkyl chain length from a C₁₀ chain to C₁₅ and C₁₈ ones is detrimental to inhibitory activity, with IC₅₀ decreasing by a factor of 12 and 20, respectively. The introduction of an unsaturation within the alkyl chain (compounds **12d** and **12f**) leads to an inhibitory activity in the same range as that of a saturated compound (**12c**). The configuration of the double bond did not display a significant difference among the obtained IC₅₀ with IC₅₀ equal to 18.9 μM for the *Z*-unsaturated compound (**12d**), as compared to 17.3 μM for the *E*-unsaturated one (**12f**) and 15.8 μM for the saturated one (**12c**). The potential filling of the $MraY_{AA}$ hot spots (HS) by aromatic substituents was rather satisfying, with IC₅₀ in the low μM range (3.2 μM and 5.8 μM) for compounds **12e** and **12g**, respectively. The results concerning the tentative filling of two $MraY_{AA}$ HS by two substituents are contrasted. Indeed, the compound **12i** with two C₁₀ alkyl chain revealed no activity, showing that it is probably too hindered for correct positioning within the $MraY_{AA}$ active site, while the oxadiazole, with both a C₉ alkyl chain and an ethyl ester, was moderately active with an IC₅₀ equal to 27.5 μM. More interestingly, the corresponding carboxylate **12j** is almost tenfold more active (IC₅₀ equal to 2.9 μM) than the parent ester, probably due to its better positioning in the $MraY_{AA}$ active site.

The antibacterial activity of $MraY$ inhibitors **12a–12h** was also evaluated against several bacterial strains. Gram-negative (*E. coli* ATCC 8730, *C. freundii* ATCC8090 and *P. aeruginosa* ATCC 27853) and Gram-positive pathogenic bacterial strains (*S. aureus* ATCC 25923 and *E. faecium* ATCC 19434), including a methicillin-resistant strain (*S. aureus* MRSA ATCC 43300), were selected as a representative of pathogen bacterial diversity. Piperacillin and vancomycin were used as positive control in the tests. The results (See Table S1, Supplementary Material) show that, although our previous data on differently substituted

urea-containing inhibitors [41], suggested that a linear chain of at least 12 carbon atoms, or a branched substituent, is required to get antibacterial activity, almost none of the oxadiazole inhibitors displayed antibacterial activity, except a modest 50 µg/mL activity for two long-chain-containing compounds, **12c** (C₁₈) and **12f** (C₁₇ with a *E* unsaturation), on the three Gram-positive bacterial strains. This disappointing result demonstrates that the further optimization of the lipophilic side chain is still required to increase the antibacterial activity.

2.3. Docking Studies

Molecular modeling studies were performed to rationalize the SAR results for this novel series of *MraY*_{AA} inhibitors. CDOCKER [52] was used to dock the compounds into the X-ray structures of the *MraY*_{AA} enzyme in open and close conformations (PDB ID: 5CKR and PDB ID: 6OYH, respectively), following the procedure described previously [41,42]. The top 50 best docking poses, based on the CDOCKER interaction energy function, were retained and then further visually examined.

In the closed conformation of *MraY*_{AA} (PDB ID: 6OYH), compounds **12a–12d** and **12f–12h** exhibit a binding mode similar to that of triazole compound **13** (Figure 4). The uracil moiety forms an H-bond with the key residue D196 and π - π stacking interactions with F262 within the small uracil binding pocket. The lipophilic tail anchors deeply in the hydrophobic groove HS4 predicted to be the C₅₅P substrate binding pocket [38] establishing hydrophobic contacts with P322 and L191 in HS2 and HS6 pockets, respectively. In addition, an extended network of H-bond and electrostatic interactions was retrieved between the aminoribosyl part and residues N190 and D193 located in the HS1 domain. No stabilizing H-bond interactions were predicted between the oxadiazole moiety and polar residues H324 and H325 within the HS2 area. Nevertheless, docking in the closed conformation of *MraY*_{AA} failed to discriminate between active **12a** and moderately active compounds (**12b–d**, **12f–h** and **12j**). Moreover, rigid or branched tail compounds (**12e** and **12i**, respectively) failed to assume this binding mode due to steric hindrance with the residues of the active site.

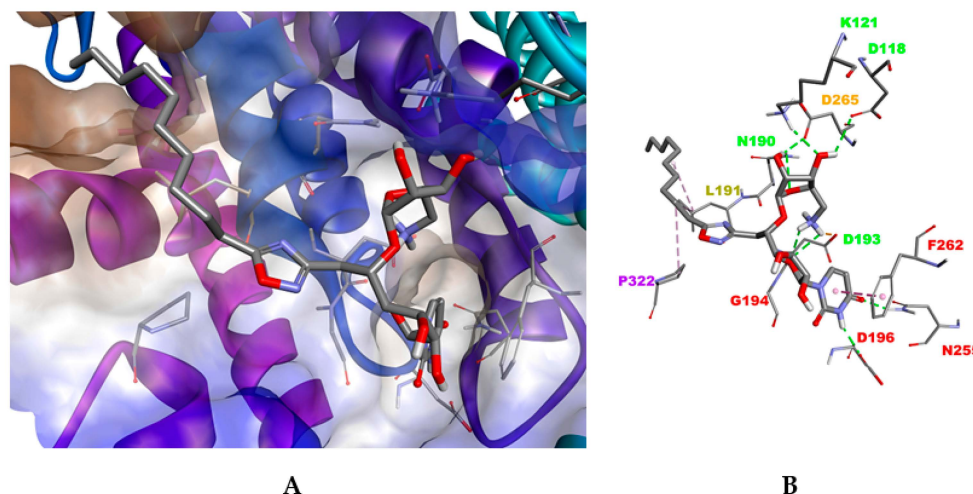


Figure 4. Docking pose for a compound in the closed conformation of *MraY*_{AA} (PDB ID: 6OYH). (A). The hydrophobic surface is rendered as brown and the hydrophilic surface as blue. Ligand and residues are shown in stick mode. (B). Interactions between the inhibitor **12a** and *MraY*_{AA} are shown as colored dashed lines: hydrophobic interactions (magenta), electrostatic interactions (orange) and hydrogen bond (green). For clarity, the apolar hydrogen atoms are omitted.

The best docking results were obtained in the open conformation of *MraY*_{AA} (PDB ID: 5CKR). Although all compounds target the uridine- and uridine-adjacent pockets, as previously seen in closed conformation, significant differences were observed in the interaction network. Two possible binding conformations (I, II) were obtained for the most active compound, **12a** (Figure 5A). Both are characterized by two new stabilizing

interactions between the uracil moiety and residues K70 and N255 but differ in the spatial orientation of the lipophilic tail, located either in the plane of the membrane (binding mode I, Figure 5B) or exposed in the cytoplasm (binding mode II, Figure 5C). Moreover, a supplementary H-bond with the residue H325 was also predicted for the oxadiazole linker, only for binding mode I. The other compounds bind to the *MraY_{AA}* active site according to the binding mode II only. For compounds **12e** and **12g**, the interactions network with the aminoribosyluridine part remained similar to that of compound **12a**. Nevertheless, the H-bond interaction of H325 with the oxadiazole moiety was lost, reducing the stability of the compound within the binding site and consequently its activity. Interestingly, the loss of this H-bond was fairly compensated by hydrophobic contacts between the lipophilic tail and residues L191 (HS6) and F309 and between A321 (HS2) and V302 (HS4).

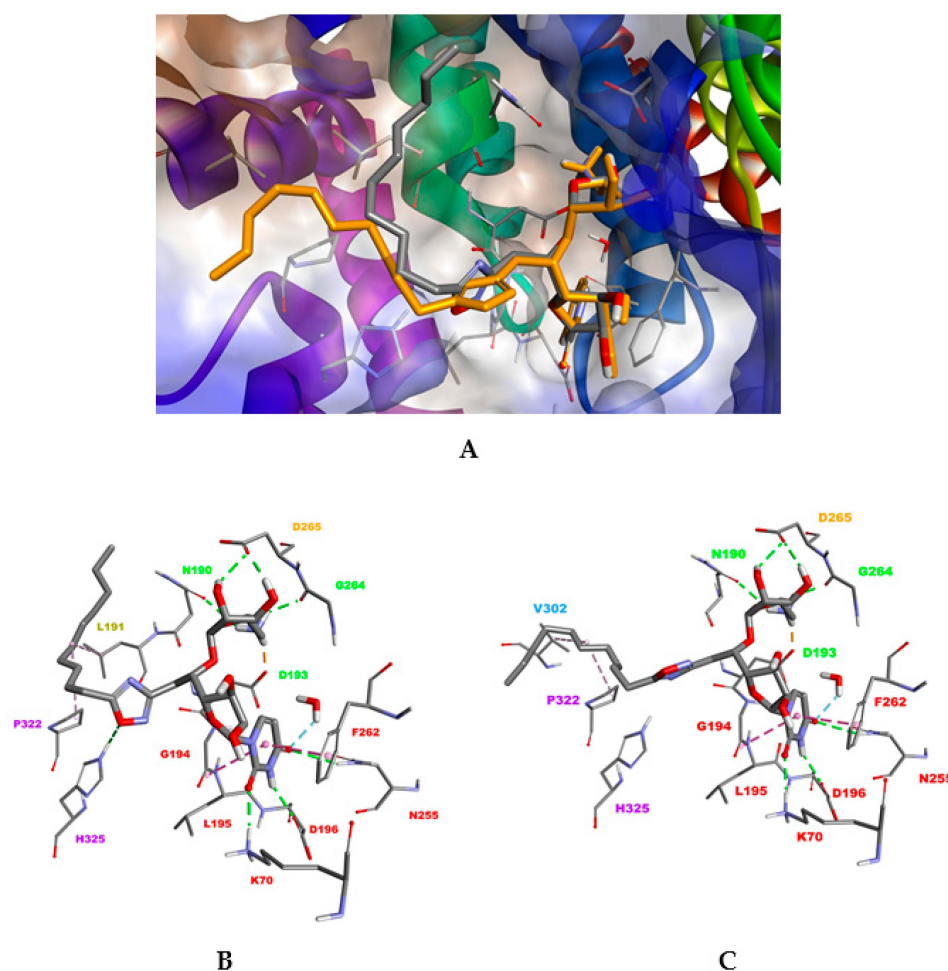


Figure 5. (A) Superimposition of the two docking conformations I and II, obtained for compound **12a** in the open conformation of *MraY_{AA}* (PDB ID: 5CKR). (B) Binding mode I. (C) Binding mode II. Ligand and residues are shown in stick mode. Interactions between the inhibitor **12a** and *MraY_{AA}* are shown as colored dashed lines: hydrophobic interactions (magenta), electrostatic interactions (orange) and hydrogen bond (green). For clarity, the apolar hydrogen atoms are omitted.

For compound **12b**, interaction with H325 seems to be detrimental to the appropriate orientation of the long hydrophobic tail within the HS2 pocket. Less active compounds **12c**, **12d** and **12f** lose at least two significant H-bonds involving N255 in the uridine binding pocket and H325 (HS2). For the branched compound **12i**, the HS2 area can accommodate only one branch, leaving the other one exposed towards the solvent surface. Concerning the compounds **2h** and **2j** with both a C9 alkyl chain and either an ethyl ester or a carboxylate moiety, no clear conclusions could be drawn from docking results. Taken together, these

results suggest that tight interactions of compound **12a** with residues within the uracil binding pocket, uridine like and HS2 domain in the open conformation of MraY_{AA} could reduce its flexibility providing an explanation for its better activity.

3. Materials and Methods

3.1. Chemical Synthesis

The reactions were carried out under an argon atmosphere, if required, and were monitored by thin-layer chromatography. All microwave-mediated reactions were carried out in G10 or G20 Anton Paar vials, using an Anton Paar Monowave 300 Extra microwave synthesizer. Flash chromatography was performed with silica gel 60 (40–63 μm). Spectroscopic ^1H and ^{13}C NMR, MS and/or analytical data were obtained using chromatographically homogeneous samples. ^1H NMR (500 MHz) and ^{13}C NMR (125 MHz) spectra were recorded in CDCl_3 unless otherwise indicated. Chemical shifts (δ) are reported in ppm, and coupling constants are given in Hz. For each compound, detailed peak assignments have been made according to COSY, HSQC and HMBC experiments. The numbering of molecules is indicated in the Supplementary Material. Optical rotations were measured with a sodium (589 nm) lamp at 20 $^\circ\text{C}$. IR spectra were recorded on an FT-IR spectrophotometer, and the wavelengths are reported in cm^{-1} . High-resolution mass spectra (HRMS) were recorded with a TOF mass analyzer under electrospray ionization (ESI) in positive ionization mode detection [42].

3.1.1. Protected Nitrile **1**

To a solution of **E** (100 mg 0.19 mmol, 1 equiv.) and **D** (192 mg, 78 mmol, 4 equiv.) in freshly distilled DCM (7 mL) was added 4 \AA molecular sieves (1.4 g). After stirring at r.t. for 1 h, boron trifluoride diethyl etherate (96 μL , 0.78 mmol, 4 equiv.) was added at -80°C . After 15 min at -80°C , the cooling bath was removed, then the mixture was allowed to warm to r.t. for 16 h. The mixture was filtrated over a pad of celite, then washed with EtOAc. The filtrate was treated with a saturated aqueous solution of sodium bicarbonate. The organic layer was washed with water and brine, then concentrated in vacuo. Flash chromatographic purification (cyclohexane/EtOAc 75:25) afforded the product as a white solid (96 mg, 67%): R_f 0.17 (cyclohexane/EtOAc 7/3); $[\alpha]_D^{+94.1}$ (c 1.0, CH_2Cl_2); IR (film) 3675, 2971, 2900, 1696, 1684, 1394, 1229, 1076, 1047, 891, 869; ^1H NMR (500 MHz, CDCl_3) δ 8.58 (br s, 1H, NH), 7.73 (d, $J_{\text{H}_6-\text{H}_5} = 8.2$ Hz, 1H, H_6), 5.74–5.53 (m, 2H, $\text{H}_5 + \text{H}_{1'}$), 5.11 (s, 1H, $\text{H}_{1''}$), 4.53 (d, $J_{\text{H}_2''-\text{H}_3''} = 6.2$ Hz, H_2''), 4.43 (d, $J_{\text{H}_3''-\text{H}_2''} = 6.2$ Hz, 1H, H_3''), 4.31 (t, $J_{\text{H}_4''-\text{H}_5''\text{b}} = J_{\text{H}_4''-\text{H}_5''\text{a}} = 5.4$ Hz, 1H, H_4''), 4.17–4.03 (m, 2H, $\text{H}_4' + \text{H}_2'$), 3.98–3.84 (m, 2H, $\text{H}_3' + \text{H}_5'$), 3.45–3.40 (m, 2H, $\text{H}_5''\text{a}$, $\text{H}_5''\text{b}$), 2.93–2.80 (m, 2H, $\text{H}_6''\text{b}$, $\text{H}_6''\text{a}$), 1.60 (q, $J = 7.4$ Hz, 2H, H_7''), 1.46 (q, $J = 7.4$ Hz, 2H, H_7''), 0.87–0.74 (m, 24H, $-\text{C}(\text{CH}_3)_3$, H_8''), 0.16–0.04 (m, 12H, $-\text{Si}(\text{CH}_3)_2$); ^{13}C NMR (125 MHz, CDCl_3) δ 162.9 (C_4), 149.95 (C_2), 140.15 (C_6), 118.12 (C_6''), 116.63 (C_7), 112.34 ($\text{C}_{1''}$), 101.56 (C_5), 90.20 ($\text{C}_{1'}$), 86.00 (C_3''), 85.49 (C_4''), 84.21 (C_4'), 81.56 (C_2''), 75.23 (C_5'), 75.05 (C_2'), 71.05 (C_3'), 53.45 (C_5''), 29.18 (C_7''), 28.85 (C_7''), 25.80 ($-\text{C}(\text{CH}_3)_3$), 21.72 (C_6'), 18.0, 17.9 ($-\text{C}(\text{CH}_3)_3$), 8.36 (C_8''), -4.0 , -4.3 , -4.9 , -4.9 ($-\text{Si}(\text{CH}_3)_2$); HRMS ESI+ Calcd. for $\text{C}_{33}\text{H}_{57}\text{N}_6\text{O}_9\text{Si}_2^+$ ($\text{M} + \text{H}$) $^+$ 737.3720, found 737.3731.

3.1.2. Protected Amidoxime **2**

The mixture of nitrile **1** (363 mg, 0.49 mmol, 1 equiv.) and 50% aqueous hydroxylamine (0.23 mL, 3.94 mmol, 8 equiv) in MeOH (8 mL) was heated at reflux for 6 h, then concentrated in vacuo. The oily residue was diluted with EtOAc (30 mL), then washed with water and brine ($2 \times 10\text{mL}$). The organic layer was dried (MgSO_4), then concentrated in vacuo. Flash chromatographic purification (cyclohexane/EtOAc 75:25) afforded product **2** as a white solid (329 mg, 87%): R_f 0.25 (cyclohexane/EtOAc = 1/1); $[\alpha]_D^{+13}$ (c 1.0, CH_2Cl_2); IR (film): 1260, 1165, 1091, 911, 834, 735. ^1H NMR (500 MHz, CDCl_3) δ 7.75 (d, $J_{\text{H}_6-\text{H}_5} = 8.1$ Hz, 1H, H_6), 5.88 (d, $J_{\text{H}_1'-\text{H}_2'} = 5.5$ Hz, 1H, $\text{H}_{1'}$), 5.73 (d, $J_{\text{H}_5-\text{H}_6} = 8.2$ Hz, 1H, H_5), 5.31 (s, 1H, $\text{H}_{1''}$), 4.62 (dd, $J_{\text{H}_3''-\text{H}_2''} = 6.3$ Hz, $J_{\text{H}_3''-\text{H}_4''} = 1.7$ Hz, 1H, H_3''), 4.53 (d, $J_{\text{H}_2''-\text{H}_3''} = 6.3$ Hz, 1H, H_2''), 4.34 (td, $J_{\text{H}_4''-\text{H}_5''} = 5.6$ Hz, $J_{\text{H}_4''-\text{H}_3''} = 1.7$ Hz, 1H, H_4''), 4.25 (t, $J_{\text{H}_5'-\text{H}_4'} = 3.0$ Hz,

1H, H_{5'}), 4.16–4.09 (m, 2H, H_{2'}, H_{4'}), 4.05 (t, $J_{H3'-H2'} = 3.8$ Hz, 1H, H_{3'}), 3.49 (dd, $J_{H6a'-H5'} = 12.8$ Hz, $J_{H6a'-H6b'} = 5.6$ Hz, 1H, H_{6a'}), 3.45 (dd, $J_{H6b'-H5'} = 12.8$ Hz, $J_{H6b'-H6a'} = 5.6$ Hz, 1H, H_{6b'}), 2.80 (dd, $J_{H5a'-H6'} = 14.3$ Hz, $J_{H5a'-H5b'} = 5.5$ Hz, 1H, H_{5a'}), 2.52 (dd, $J_{H5b'-H6'} = 14.3$ Hz, $J_{H5b'-H5a'} = 8.8$ Hz, 1H, H_{5b'}), 1.69 (q, $J_{H7a''-H8''} = 7.4$ Hz, 2H, H_{7a''}), 1.55 (q, $J_{H7b''-H8''} = 7.5$ Hz, 2H, H_{7b''}), 0.91–0.83 (m, 24H, H_{8''}, Si(CH₃)₃), 0.10–0.02 (m, 12H, Si(CH₃)₂). ¹³C NMR (125 MHz, CDCl₃) δ 171.8 (C_{7'}), 162.8 (C₄), 150.1 (C₂), 140.5 (C₆), 111.8 (C_{1''}), 102.1 (C₅), 89.0 (C_{1'}), 86.2 (C_{2''}), 86.1 (C_{4'}), 84.8 (C_{4'}), 81.5 (C_{5'}), 75.3 (C_{2'}), 72.3 (C_{3'}), 53.6 (C_{5''}), 38.7 (C_{6'ab}), 29.4 (C_{7''}), 29.0 (C_{7''}), 25.93, 25.86 (–C(CH₃)₃), 18.1 (–C(CH₃)₃), 8.5, 7.7 (C_{8''}), –4.1, –4.6, –4.8, (–SiC); HRMS ESI+ calcd. for C₃₃H₆₀N₇O₁₀Si₂⁺ (M + H)⁺ 770.3935 found 770.3914.

3.1.3. General Procedure for the Synthesis of Protected Oxadiazoles

In a 10 mL microwave reaction vial, to a solution of amidoxime **2** (1 equiv.) in toluene (3 mL) was added acyl chloride **3a–3i** (1.1 equiv.) and DBU (2.5 equiv.). The reaction was stirred at r.t. for 30 min. Then the reaction mixture was irradiated under microwave irradiation at 150 °C for 30 min to 1 h. The reaction mixture was then concentrated in vacuo. Flash chromatographic purifications (cyclohexane/EtOAc 9:1) afforded the products **11a–11i** in 42 to 83% yield.

3.1.4. Protected Oxadiazole **11a**

Compound **11a** was obtained as a white solid (40 mg, 67% yield): R_f 0.25 (cyclohexane/EtOAc = 7/3); [α]_D +14 (c 1.0, CH₂Cl₂); IR (film): 3006, 2873, 1558, 1427, 1368, 1275, 1146, 1016, 988, 935, 887, 820, 764, 750; ¹H NMR (500 MHz, CDCl₃) δ 7.89 (d, $J_{H6-H5} = 8.2$ Hz, 1H, H₆), 5.85 (d, $J_{H1'-H2'} = 4.7$ Hz, 1H, H_{1'}), 5.73 (dd, $J_{H5-H6} = 8.2$ Hz, 1H, H₅), 5.24 (s, 1H, H_{1''}), 4.64 (dd, $J_{H3''-H2''} = 6.2$ Hz, $J_{H3''-H4''} = 1.5$ Hz, 1H, H_{3''}), 4.52 (d, $J_{H2''-H3''} = 6.2$ Hz, 1H, H_{2''}), 4.32 (t, $J_{H5'-H4'} = 5.8$ Hz, 1H, H_{5'}), 4.24–4.21 (m, 1H, H_{4''}), 4.16 (t, $J_{H2'-H3'} = 4.7$ Hz, 1H, H_{2'}), 4.05 (dd, $J_{H4'-H3'} = 4.4$ Hz, $J_{H4'-H5'} = 1.6$ Hz, 1H, H_{4'}), 3.99 (t, $J_{H3'-H4'} = 4.4$ Hz, 1H, H_{3'}), 3.50 (dd, $J_{H6'a-H5'} = 12.7$ Hz, $J_{H6'a-H6'b} = 5.2$ Hz, 1H, H_{6'a}), 3.43 (dd, $J_{H6'b-H5'} = 12.7$ Hz, $J_{H6'b-H5'} = 5.2$ Hz, 1H, H_{6'b}), 3.38 (dd, $J_{H5''a-H4''} = 15.0$ Hz, $J_{H5''a-H5''b} = 9.3$ Hz, 1H, H_{5''a}), 3.19 (dd, $J_{H5''b-H4''} = 15.0$ Hz, $J_{H5''b-H5''a} = 9.3$ Hz, 1H, H_{5''b}), 2.83 (t, $J_{H2'-H3'} = 7.6$ Hz, 1H, H_{1*}), 1.80–1.74 (m, 2H, H_{2*}), 1.69 (q, $J_{H7''-H8''} = 7.5$ Hz, 2H, H_{7''}), 1.56 (q, $J_{H7''-H8''} = 7.5$ Hz, 2H, H_{7''}), 1.30–1.24 (m, 24H, H_{3*-H14*}), 0.92–0.82 (m, 27H, –SiC(CH₃)₃, H_{8''}, H_{15*}), 0.08–0.05 (12H, Si(CH₃)₂); ¹³C NMR (125 MHz, CDCl₃) δ 180.2 (C_{8'}), 166.9 (C_{7'}), 163.0 (C₄), 150.1 (C₂), 140.2 (C₆), 118.00 (C_{6''}), 112.2 (C_{1''}), 101.8 (C₅), 88.7 (C_{1'}), 86.1 (C_{2''}), 85.0 (C_{4''}), 84.6 (C_{4'}), 81.7 (C_{3''}), 78.2 (C_{5'}), 75.5 (C_{2'}), 72.0 (C_{3'}), 53.4 (C_{5''}), 31.9, 29.6, 29.4, 29.3, 29.2, 29.1, 28.9, 25.8 (C_{2*-C9*}), 26.6, 26.5 (C_{6'}, C_{1*}), 25.76 (SiCCH₃), 22.69 (s), 18.0 (SiCCH₃), 14.1 (C_{10*}), 8.4, 7.5 (C_{8''}), –4.2, –4.5, –4.8 (SiCH₃); HRMS ESI+ calcd. for C₄₄H₇₈N₇O₁₀Si₂⁺ (M + H)⁺ 920.5343 found 920.5326.

3.1.5. Protected Oxadiazole **11b**

Compound **11b** was obtained as a white solid (53 mg, 55% yield): R_f 0.25 (cyclohexane/EtOAc = 7/3); [α]_D +10 (c 1.0, CH₂Cl₂); IR (film): 3006, 2873, 1558, 1427, 1368, 1275, 1146, 1016, 988, 935, 887, 820, 764, 750; ¹H NMR (500 MHz, CDCl₃) δ 8.61 (s, 1H, NH), 7.88 (d, $J_{H5-H6} = 8.1$ Hz, 1H, H₆), 5.84 (d, $J_{H1'-H2'} = 4.3$ Hz, 1H, H_{1'}), 5.72 (d, $J_{H5-H6} = 8.1$ Hz, 1H, H₅), 5.24 (s, 1H, H_{1''}), 4.63 (d, $J_{H2''-H3''} = 6.1$ Hz, 1H, H_{3''}), 4.52 (d, $J_{H2''-H3''} = 6.0$ Hz, 1H, H_{2''}), 4.33–4.29 (m, 1H, H_{4''}), 4.26–4.19 (m, 1H, H_{5'}), 4.18–4.14 (m, 1H, H_{2'}), 4.05 (d, $J_{H3'-H4'} = 3.0$ Hz, 1H, H_{4'}), 4.00 (d, $J_{H3'-H4'} = 3.0$ Hz, 1H, H_{3'}), 3.50 (dd, $J_{H5''a-H5''b} = 12.9$ Hz, $J_{H4''-H5''a} = 5.1$ Hz, 1H, H_{5''a}), 3.42 (dd, $J_{H5''a-H5''b} = 12.9$ Hz, $J_{H4''-H5''b} = 5.8$ Hz, 1H, H_{5''b}), 3.37 (dd, $J_{H6'a-H6'b} = 14.9$ Hz, $J_{H6'a-H5'} = 5.0$ Hz, 1H, H_{6'a}), 3.19 (dd, $J_{H6'a-H6'b} = 14.9$ Hz, $J_{H6'b-H5'} = 9.2$ Hz, 1H, H_{6'b}), 2.82 (t, $J_{H1*-H2*} = 7.6$ Hz, 2H, H_{1*}), 1.84–1.62 (m, 4H, H_{2*}, H_{7''}), 1.56 (q, $J_{H7''-H8''} = 7.2$ Hz, 2H, H_{7''}), 1.40–1.17 (m, 16H, H_{2*-H9*}), 0.97–0.75 (m, 21H, H_{10*}, H_{8''}, SiC(CH₃)₃), 0.07, 0.07, 0.06 (s, 12H, SiCH₃); ¹³C NMR (125 MHz, CDCl₃) δ 180.3 (C_{8'}), 166.9 (C_{7'}), 162.9 (C₄), 150.0 (C₂), 140.3 (C₆), 118.1 (C_{6''}), 112.3 (C_{1''}), 101.8 (C₅), 88.8 (C_{1'}), 86.1 (C_{2''}), 85.0 (C_{4''}), 84.7 (C_{4'}), 81.7 (C_{3''}), 78.3 (C_{5'}), 75.5 (C_{2'}), 72.1 (C_{3'}), 53.4 (C_{6'ab}), 32.0 (C_{4*}), 29.8, 29.7, 29.5 (C_{5''b}), 29.3, 29.3, 29.2 (C_{5''a}), 29.1 (C_{7''}), 28.9 (C_{7''}), 26.7 (C_{1*}), 26.6 (C_{2*}),

25.9 (SiC(CH₃)₃), 25.8 (SiC(CH₃)₃), 22.8 (C₃*), 18.0 (C₁₄*), 14.2 (C₁₅*), 8.5 (C₈"), 7.6 (C₃"), -4.0 (SiCH₃), -4.4 (SiCH₃), -4.6 (SiC), -4.7 (SiC). HRMS ESI+ calcd. for C₄₉H₈₈N₇O₁₀Si₂⁺ (M + H)⁺ 990.6125 found 990.6105.

3.1.6. Protected Oxadiazole 11c

Compound **11c** was obtained as a colorless oil (50 mg, 75% yield): R_f 0.25 (cyclohexane/EtOAc = 7/3); [α]_D +16 (c 1.0, CH₂Cl₂); IR (film): 2926, 2855, 2105, 1695, 1462, 1378, 1275, 1167, 1100, 925, 867, 839, 764, 750; ¹H NMR (500 MHz, CDCl₃) δ 7.89 (d, J_{H6-H5} = 8.0 Hz, 1H, H₆), 5.85 (d, J_{H1'-H2'} = 4.4 Hz, 1H, H_{1'}), 5.73 (dd, J_{H5-H6} = 8.0 Hz, J_{H5-H1'} = 2.2 Hz, 1H, H₅), 5.24 (s, 1H, H₁"), 4.64 (dd, J_{H3"-H2"} = 6.6 Hz, J_{H3"-H4"} = 1.4 Hz, 1H, H₃"), 4.51 (d, J_{H2"-H3"} = 6.5 Hz, 1H, H₂"), 4.32 (t, J_{H5'-H4'} = 5.7 Hz, 1H, H_{5'}), 4.24–4.21 (m, 1H, H₄"), 4.16 (t, J_{H2'-H3'} = 4.4 Hz, 1H, H_{2'}), 4.05 (dd, J_{H4'-H3'} = 4.2 Hz, J_{H4'-H5'} = 1.5 Hz, 1H, H_{4'}), 3.98 (t, J_{H3'-H4'} = 4.2 Hz, 1H, H_{3'}), 3.50 (dd, J_{H6'a-H5'} = 12.8 Hz, J_{H6'a-H6'b} = 5.8 Hz, 1H, H_{6'a}), 3.43 (dd, J_{H6'b-H5'} = 12.8 Hz, J_{H6'b-H5'} = 5.8 Hz, 1H, H_{6'b}), 3.38 (dd, J_{H5"a-H4"} = 15.0 Hz, J_{H5"a-H5"b} = 9.3 Hz, 1H, H_{5"a}), 3.19 (dd, J_{H5"b-H4"} = 15.0 Hz, J_{H5"b-H5"a} = 9.3 Hz, 1H, H_{5"b}), 2.83 (t, J_{H2'-H3'} = 7.6 Hz, 1H, H₁*), 1.79–1.73 (m, 2H, H₂*), 1.69 (q, J_{H7"-H8"} = 7.4 Hz, 2H, H₇"), 1.56 (q, J_{H7"-H8"} = 7.4 Hz, 2H, H₇"), 1.38–1.24 (m, 30H, H₃*-H₁₇*), 0.92–0.84 (m, 27H, SiC(CH₃)₃, H₈", H₁₈*), 0.07–0.05 (12H, Si(CH₃)₂); ¹³C NMR (125 MHz, CDCl₃) δ 180.1 (C_{8'}), 166.8 (C_{7'}), 162.8 (C₄), 149.9 (C₂), 140.1 (C₆), 117.9 (C₆"), 112.1 (C₁"), 101.6 (C₅), 88.6 (C₁'), 85.9 (C₂"), 84.9 (C₄"), 84.5 (C_{4'}), 81.6 (C₃"), 78.1 (C₅'), 75.4 (C₂'), 71.9 (C₃'), 53.2 (C_{6'}ab), 31.9 (C₄*), 29.6, 29.3, 29.3 (C₅"b), 29.2, 29.1, 29.1 (C₅"a), 29.0 (C₇"'), 28.7 (C₇"'), 26.6 (C₁*), 26.4 (C₂*), 25.7 (SiC(CH₃)₃), 25.6 (SiC(CH₃)₃), 22.6 (C₃*), 17.9 (C₁₇*), 14.1 (C₁₈*), 8.3 (C₈"), 7.4 (C₈"), -4.2 (SiCH₃), -4.5 (SiCH₃), -4.8 (SiC), -4.8 (SiC); HRMS ESI+ calcd. for C₅₂H₉₄N₇O₁₀Si₂⁺ (M + H)⁺ 1032.6595 found 1032.6576.

3.1.7. Protected Oxadiazole 11d

Compound **11d** was obtained as a colorless oil (47.5 mg, 72% yield): R_f 0.25 (cyclohexane/EtOAc = 7/3); [α]_D +33 (c 1.0, CH₂Cl₂); IR (film): 2928, 2856, 2105, 1695, 1462, 1378, 1275, 1167, 1099, 924, 903, 867, 838, 764, 750; ¹H NMR (500 MHz, CDCl₃) δ 7.89 (d, J_{H6-H5} = 8.2 Hz, 1H, H₆), 5.85 (d, J_{H1'-H2'} = 4.7 Hz, 1H, H_{1'}), 5.73 (d, J_{H5-H6} = 8.2 Hz, 1H, H₅), 5.35–5.30 (m, 2H, H₈*, H₉*), 5.24 (s, 1H, H₁"), 4.64 (dd, J_{H3"-H2"} = 6.2 Hz, J_{H3"-H4"} = 1.5 Hz, 1H, H₃"), 4.52 (d, J_{H2"-H3"} = 6.5 Hz, 1H, H₂"), 4.31 (t, J_{H5'-H4'} = 5.8 Hz, 1H, H_{5'}), 4.24–4.21 (m, 1H, H₄"), 4.15 (t, J_{H2'-H3'} = 4.5 Hz, 1H, H_{2'}), 4.05 (dd, J_{H4'-H3'} = 4.2 Hz, J_{H4'-H5'} = 1.6 Hz, 1H, H_{4'}), 3.98 (t, J_{H3'-H4'} = 4.3 Hz, 1H, H_{3'}), 3.50 (dd, J_{H6'a-H5'} = 13.0 Hz, J_{H6'a-H6'b} = 5.2 Hz, 1H, H_{6'a}), 3.43 (dd, J_{H6'b-H5'} = 13.0 Hz, J_{H6'b-H5'} = 5.8 Hz, 1H, H_{6'b}), 3.38 (dd, J_{H5"a-H4"} = 15.0 Hz, J_{H5"a-H5"b} = 9.2 Hz, 1H, H_{5"a}), 3.19 (dd, J_{H5"b-H4"} = 15.0 Hz, J_{H5"b-H5"a} = 9.2 Hz, 1H, H_{5"b}), 2.84 (t, J_{H2'-H3'} = 7.8 Hz, 1H, H₁*), 2.02–1.98 (m, 4H, H₇*, H₁₀*), 1.80–1.74 (m, 2H, H₂*), 1.69 (q, J_{H7"-H8"} = 7.4 Hz, 2H, H₇"), 1.56 (q, J_{H7"-H8"} = 7.4 Hz, 2H, H₇"), 1.42–1.24 (m, 20H, H₃*-H₆*, H₉*-H₁₆*), 0.92–0.84 (m, 27H, -SiC(CH₃)₃, H₈", H₁₇*), 0.07–0.05 (12H, Si(CH₃)₂); ¹³C NMR (125 MHz, CDCl₃) δ 180.2 (C_{8'}), 166.9 (C_{7'}), 163.0 (C₄), 150.0 (C₂), 140.2 (C₆), 130.2 (C₈*), 129.7 (C₉*), 118.0 (C₆"), 112.3 (C₁"), 101.8 (C₅), 88.8 (C₁'), 86.1 (C₂"), 85.0 (C₄"), 84.7 (C_{4'}), 81.7 (C₃"), 78.3 (C₅'), 75.5 (C₂'), 72.0 (C₃'), 53.4 (C_{6'}ab), 32.0 (C₄*), 29.9, 29.8 (C₅"b), 29.6, 29.4, 29.3 (C₅"a), 29.1 (C₇"'), 28.9 (C₇"'), 27.3 (C₇*), 27.2 (C₁₀*), 26.7 (C₁*), 26.6 (C₂*), 25.9 (SiC(CH₃)₃), 25.8 (SiC(CH₃)₃), 22.8 (C₃*), 18.1 (C₁₆*), 14.2 (C₁₇*), 8.5 (C₈"), 7.6 (C₈"), -4.0 (SiCH₃), -4.4 (SiCH₃), -4.6 (SiC), -4.7 (SiC); HRMS ESI+ calcd. for C₅₁H₉₀N₇O₁₀Si₂⁺ (M + H)⁺ 1016.6282 found 1016.6258.

3.1.8. Protected Oxadiazole 11e

Compound **11e** was obtained as a colorless oil (23 mg, 42% yield): R_f 0.25 (cyclohexane/EtOAc = 7/3); [α]_D +33 (c 1.0, CH₂Cl₂); IR (film): 2930, 2106, 1697, 1487, 1368, 1275, 1275, 1168, 1100, 924, 870, 839, 764, 750; ¹H NMR (500 MHz, CDCl₃) δ 8.06 (d, J_{Ha-Hb} = 8.8 Hz, 2H, H_a), 7.91 (dd, J_{H6-H5} = 8.3 Hz, J_{H6-H1'} = 3.3 Hz, 1H, H₆), 7.41 (t, J_{Hd-He} = 7.9 Hz, 2H, H_d), 7.22 (t, J_{He-Hd} = 7.4 Hz, 1H, H_e), 7.09 (d, J_{Hd-Hc} = 8.8 Hz, 2H, H_c), 7.07 (d, J_{Hb-Ha} = 8.8 Hz, 2H, H_b), 5.85 (d, J_{H1'-H2'} = 4.4 Hz, 1H, H_{1'}), 5.74 (dd, J_{H5-H6} = 8.3 Hz, J_{H5-H1'} =

2.0 Hz, 1H, H₅), 5.29 (s, 1H, H_{1''}), 4.65 (dd, $J_{H3''-H2''} = 6.2$ Hz, $J_{H3''-H4''} = 1.5$ Hz, 1H, H_{3''}), 4.54 (d, $J_{H2''-H3''} = 6.2$ Hz, 1H, H_{2''}), 4.32–4.21 (m, 2 H, H_{5'}, H_{4''}), 4.18–4.14 (m, 2 H, H_{2'}, H_{4'}), 4.01 (t, $J_{H3'-H4'} = 4.2$ Hz, 1H, H_{3'}), 3.52 (dd, $J_{H6'a-H5'} = 12.8$ Hz, $J_{H6'a-H6'b} = 5.5$ Hz, 1H, H_{6'a}), 3.47–3.42 (m, 2 H, H_{6'b}, H_{5''a}), 3.27 (dd, $J_{H5''b-H4''} = 15.0$ Hz, $J_{H5''b-H5''a} = 9.2$ Hz, 1H, H_{5''b}), 1.70 (q, $J_{H7''-H8''} = 7.4$ Hz, 2 H, H_{7''}), 1.56 (q, $J_{H7''-H8''} = 7.4$ Hz, 2 H, H_{7''}), 0.92–0.82 (m, 24H, -SiC(CH₃)₃, H_{8''}), 0.07–0.05 (12 H, Si(CH₃)₂); ¹³C NMR (125 MHz, CDCl₃) δ 175.4 (C_{8'}), 167.6 (C_{7'}), 161.9 (C₄), 155.4 (C_{10'}), 150.0 (C₂), 130.2 (C_a, C_d), 124.9 (C_e), 120.3 (C_c), 118.3 (C_b), 118.1 (C_{6''}), 112.2 (C_{1''}), 101.8 (C₅), 88.8 (C_{1'}), 86.1 (C_{2''}), 85.0 (C_{4''}), 84.8 (C_{4'}), 81.7 (C_{3''}), 78.2 (C_{5'}), 75.5 (C_{2'}), 72.1 (C_{3'}), 53.4 (C_{6'ab}), 32.0 (C_{4*}), 29.9 (C_{5''ab}), 29.3 (C_{7''}), 28.9 (C_{7''}), 25.8 (SiC(CH₃)₃), 25.8 (SiC(CH₃)₃), 18.1, 18.0 (C₉), 8.5 (C_{8''}), 7.6 (C_{8''}), -4.0 (SiCH₃), -4.4 (SiCH₃), -4.6 (SiC), -4.7 (SiC). HRMS ESI+ calcd. for C₄₆H₆₆N₇O₁₁Si₂⁺ (M + H)⁺ 948.4353 found 948.4329.

3.1.9. Protected Oxadiazole 11f

Compound **11f** was obtained as a colorless oil (55 mg, 83% yield): R_f 0.25 (cyclohexane/EtOAc = 7/3); [α]_D +15 (c 1.0, CH₂Cl₂); IR (film): 2928, 2856, 2105, 1696, 1580, 1462, 1378, 1274, 1167, 1099, 967, 910, 867, 838, 764, 748; ¹H NMR (500 MHz, CDCl₃) δ 7.89 (d, $J_{H6-H5} = 8.2$ Hz, 1H, H₆), 5.84 (d, $J_{H1'-H2'} = 4.4$ Hz, 1H, H_{1'}), 5.73 (dd, $J_{H5-H6} = 8.2$ Hz, $J_{H5-H1'} = 2.0$ Hz, 1H, H₅), 5.42–5.33 (m, 2 H, H_{8*}, H_{9*}), 5.24 (s, 1H, H_{1''}), 4.63 (dd, $J_{H3''-H2''} = 6.2$ Hz, $J_{H3''-H4''} = 1.6$ Hz, 1H, H_{3''}), 4.51 (d, $J_{H2''-H3''} = 6.0$ Hz, 1H, H_{2''}), 4.31 (t, $J_{H5'-H4'} = 5.7$ Hz, 1H, H_{5'}), 4.24–4.20 (m, 1H, H_{4''}), 4.15 (t, $J_{H2'-H3'} = 4.5$ Hz, 1H, H_{2'}), 4.05 (dd, $J_{H4'-H3'} = 4.1$ Hz, $J_{H4'-H5'} = 1.7$ Hz, 1H, H_{4'}), 3.98 (t, $J_{H3'-H4'} = 4.4$ Hz, 1H, H_{3'}), 3.50 (dd, $J_{H6'a-H5'} = 12.6$ Hz, $J_{H6'a-H6'b} = 5.1$ Hz, 1H, H_{6'a}), 3.43 (dd, $J_{H6'b-H5'} = 12.6$ Hz, $J_{H6'b-H5'} = 6.1$ Hz, 1H, H_{6'b}), 3.38 (dd, $J_{H5''a-H4''} = 14.7$ Hz, $J_{H5''a-H5''b} = 9.0$ Hz, 1H, H_{5''a}), 3.19 (dd, $J_{H5''b-H4''} = 15.0$ Hz, $J_{H5''b-H5''a} = 9.0$ Hz, 1H, H_{5''b}), 2.83 (t, $J_{H2'-H3'} = 7.7$ Hz, 1H, H_{1*}), 1.97–1.94 (m, 4 H, H_{7*}, H_{10*}), 1.80–1.73 (m, 2 H, H_{2*}), 1.70 (q, $J_{H7''-H8''} = 7.6$ Hz, 2 H, H_{7''}), 1.56 (q, $J_{H7''-H8''} = 7.6$ Hz, 2 H, H_{7''}), 1.32–1.25 (m, 20 H, H_{3*}-H_{6*}, H_{9*}-H_{16*}), 0.92–0.84 (m, 27H, -SiC(CH₃)₃, H_{8''}, H_{17*}), 0.07–0.05 (12 H, Si(CH₃)₂). ¹³C NMR (125 MHz, CDCl₃) δ 180.2 (C_{8'}), 166.9 (C_{7'}), 162.9 (C₄), 150.0 (C₂), 140.2 (C₆), 130.6 (C_{8*}), 130.2 (C_{9*}), 118.0 (C_{6''}), 112.3 (C_{1''}), 101.8 (C₅), 88.8 (C_{1'}), 86.1 (C_{2''}), 85.0 (C_{4''}), 84.7 (C_{4'}), 81.7 (C_{3''}), 78.3 (C_{5'}), 75.5 (C_{2'}), 72.0 (C_{3'}), 53.4 (C_{6'ab}), 32.7 (C_{7*}), 32.6 (C_{10*}), 32.0 (C_{4*}), 29.7, 29.6 (C_{5''b}), 29.5, 29.4, 29.3 (C_{5''a}), 29.1 (C_{7''}), 28.9 (C_{7''}), 26.7 (C_{1*}), 26.6 (C_{2*}), 25.9 (SiC(CH₃)₃), 25.8 (SiC(CH₃)₃), 22.8 (C_{3*}), 18.1 (C_{16*}), 14.2 (C_{17*}), 8.5 (C_{8''}), 7.6 (C_{8''}), -4.0 (SiCH₃), -4.4 (SiCH₃), -4.6 (SiC), -4.7 (SiC); HRMS ESI+ calcd. for C₅₁H₉₀N₇O₁₀Si₂⁺ (M + H)⁺ 1016.6282 found 1016.6274.

3.1.10. Protected Oxadiazole 11g

Compound **11g** was obtained as a colorless oil (38 mg, 58% yield): R_f 0.25 (cyclohexane/EtOAc = 7/3); [α]_D +6 (c 1.0, CH₂Cl₂); IR (film): 2929, 2856, 2105, 1695, 1580, 1462, 1377, 1274, 1167, 1100, 924, 865, 839, 764, 750; ¹H NMR (500 MHz, CDCl₃) δ 7.89 (d, $J_{H6-H5} = 8.1$ Hz, 1H, H₆), 7.28–7.16 (m, 5 H, H_{abc}), 5.85 (d, $J_{H1'-H2'} = 4.7$ Hz, 1H, H_{1'}), 5.73 (dd, $J_{H5-H6} = 8.1$ Hz, $J_{H5-H1'} = 2.0$ Hz, 1H, H₅), 5.24 (s, 1H, H_{1''}), 4.64 (dd, $J_{H3''-H2''} = 6.1$ Hz, $J_{H3''-H4''} = 1.4$ Hz, 1H, H_{3''}), 4.52 (d, $J_{H2''-H3''} = 6.1$ Hz, 1H, H_{2''}), 4.32 (t, $J_{H5'-H4'} = 5.7$ Hz, 1H, H_{5'}), 4.24–4.21 (m, 1H, H_{4''}), 4.16 (t, $J_{H2'-H3'} = 4.4$ Hz, 1H, H_{2'}), 4.05 (dd, $J_{H4'-H3'} = 4.3$ Hz, $J_{H4'-H5'} = 1.7$ Hz, 1H, H_{4'}), 3.98 (t, $J_{H3'-H4'} = 4.5$ Hz, 1H, H_{3'}), 3.50 (dd, $J_{H6'a-H5'} = 12.8$ Hz, $J_{H6'a-H6'b} = 5.8$ Hz, 1H, H_{6'a}), 3.43 (dd, $J_{H6'b-H5'} = 12.8$ Hz, $J_{H6'b-H5'} = 5.8$ Hz, 1H, H_{6'b}), 3.38 (dd, $J_{H5''a-H4''} = 15.0$ Hz, $J_{H5''a-H5''b} = 9.3$ Hz, 1H, H_{5''a}), 3.19 (dd, $J_{H5''b-H4''} = 15.0$ Hz, $J_{H5''b-H5''a} = 9.3$ Hz, 1H, H_{5''b}), 2.82 (t, $J_{H2'-H3'} = 7.6$ Hz, 1H, H_{1*}), 2.59 (t, $J_{H9'-H10'} = 7.6$ Hz, 1H, H_{9*}), 1.79–1.73 (m, 2H, H_{2*}), 1.70 (q, $J_{H7''-H8''} = 7.6$ Hz, 2 H, H_{7''}), 1.63–1.58 (m, 2H, H_{8*}), 1.56 (q, $J_{H7''-H8''} = 7.6$ Hz, 2H, H_{7''}), 1.36–1.26 (m, 10 H, H_{3*}-H_{7*}), 0.92–0.84 (m, 24H, -SiC(CH₃)₃, H_{8''}, H_{18*}), 0.07–0.05 (12 H, Si(CH₃)₂); ¹³C NMR (125 MHz, CDCl₃) δ 180.2 (C_{8'}), 166.9 (C_{7'}), 162.9 (C₄), 150.0 (C₂), 142.9 (C_{10*}), 140.2 (C₆), 128.5 (C_a), 128.3 (C_b), 125.7 (C_c), 118.0 (C_{6''}), 112.3 (C_{1''}), 101.8 (C₅), 88.8 (C_{1'}), 86.1 (C_{2''}), 85.0 (C_{4''}), 84.7 (C_{4'}), 81.7 (C_{3''}), 78.3 (C_{5'}), 75.5 (C_{2'}), 72.0 (C_{3'}), 53.4 (C_{6'ab}), 36.1 (C_{9*}), 31.6 (C_{4*}), 29.5, 29.4, 29.4 (C_{5''b}), 29.3, 29.3, 29.2 (C_{5''a}), 29.1 (C_{7''}), 28.9 (C_{7''}), 26.7 (C_{1*}), 26.6 (C_{2*}), 25.9 (SiC(CH₃)₃), 25.8 (SiC(CH₃)₃),

17.9 (C₈*), 8.5 (C₈''), 7.6 (C₈''), −4.0 (SiCH₃), −4.4 (SiCH₃), −4.6 (SiC), −4.7 (SiC). HRMS ESI− calcd. for C₄₉H₇₈N₇O₁₀Si₂[−] (M + H)[−] 980.5354 found 980.5297.

3.1.11. Protected Oxadiazole 11h

Compound **11h** was obtained as a colorless oil and as a 1/1 mixture of stereoisomers (38 mg, 58% yield): R_f 0.25 (cyclohexane/EtOAc = 7/3); [α]_D +6 (c 1.0, CH₂Cl₂); IR (film): 2929, 2856, 2105, 1695, 1580, 1462, 1377, 1274, 1167, 1100, 924, 865, 839, 764, 750; ¹H NMR (500 MHz, CDCl₃) δ 7.90 (d, J_{H5-H6} = 8.1 Hz, 1H, H₆), 5.85 (d, J_{H1'-H2'} = 3.1 Hz, 0.5H, H_{1'}), 5.84 (d, J_{H1'-H2'} = 3.4 Hz, 0.5H, H_{1'}), 5.74 (d, J_{H5-H6} = 8.1 Hz, 1H, H₅), 5.22 (s, 0.5H, H_{1''}), 5.22 (s, 0.5 H, H_{1''}), 4.63 (d, J_{H2''-H3''} = 6.1 Hz, 1H, H_{3''}), 4.51 (d, J_{H2''-H3''} = 6.1 Hz, 1H, H_{2''}), 4.35–4.23 (m, 2H, H_{4'}, H_{5'}), 4.23–4.14 (m, 3 H, H_{3**}, H_{2'}), 4.08 (dd, J_{H4'-H5'} = 8.5 Hz, J_{H3'-H4'} = 4.4 Hz, 0.5H, H_{4'}), 4.07 (dd, J_{H4'-H5'} = 8.5 Hz, J_{H3'-H4'} = 4.4 Hz, 0.5 H, H_{4'}), 4.00 (t, J_{H3'-H4'} = J_{H2'-H3'} = 4.4 Hz, 1H, H_{3'}), 3.95 (t, J = 7.6 Hz, 1H, H_{1*}), 3.50 (dd, J_{H5''a-H5''b} = 12.7, J_{H4''-H5''a} = 4.9 Hz, 0.5H, H_{5''a}), 3.49 (dd, J_{H5''a-H5''b} = 12.7, J_{H4''-H5''a} = 4.9 Hz, 0.5H, H_{5''a}), 3.46–3.34 (m, 2 H, H_{6'a}, H_{5''b}), 3.26–3.16 (m, 1H, H_{6'b}), 2.18–1.96 (m, 2 H, H_{2*}), 1.75–1.65 (m, 2H, H_{7''}), 1.59–1.51 (m, 2H, H_{7''}), 1.40–1.5 (m, 17H, H_{3*-H9*}, H_{4**}), 0.94–0.78 (m, 21 H, H_{10*}, H_{8''}, SiC(CH₃)₃), 0.07, 0.07, 0.06 (s, 12H, SiCH₃); ¹³C NMR (125 MHz, CDCl₃) δ 176.74, 176.67 (C_{2**}), 168.66, 168.63 (C_{8'}), 167.23, 167.20 (C_{7'}), 162.9, 162.8 (C₄), 150.00, 149.95 (C₂), 140.2 (C₆), 117.96, 117.93 (C_{6''}), 112.34, 112.29 (C_{1''}), 101.76 (C₅), 88.81 (C_{1'}), 86.03 (C_{2''}), 84.98, 84.86 (C_{4'}, C_{4''}), 81.7 (C_{3''}), 78.2, 78.1 (C_{5'}), 75.5 (C_{2'}), 71.9 (C_{3'}), 62.02 (C_{3**}), 53.27, 53.25 (C_{5''}), 44.60, 44.55 (C_{1*}), 31.89 (C_{2*}), 30.2, 29.7, 29.5, 29.4, 29.3, 29.2, 29.1, 28.8, 27.20, 22.7 (C_{3*-C9*}, C_{7''}), 25.81, 25.76 (SiC(CH₃)₃), 18.0 (SiC(CH₃)₃), 14.15, 14.12 (C_{4**}), 8.4, 7.5 (C_{8''}), −4.2, −4.5, −4.8 (SiCH₃); HRMS ESI− calcd. for C₄₇H₈₀N₇O₁₂Si₂[−] (M + H)[−] 990.5409 found 990.5455.

3.1.12. Protected Oxadiazole 11i

Compound **11i** was obtained as a colorless oil (57 mg, 74% yield): R_f 0.25 (cyclohexane/EtOAc = 7/3); [α]_D +10 (c 1.0, CH₂Cl₂); IR (film): 2928, 2856, 1697, 1463, 1260, 1168, 1102, 840, 779, 740; ¹H NMR (500 MHz, CDCl₃) δ 7.93 (d, J_{H6-H5} = 8.5 Hz, 1H, H₆), 5.83 (d, J_{H1'-H2'} = 4.3 Hz, 1H, H_{1'}), 5.73 (dd, J_{H5-H6} = 8.3 Hz, J_{H5-H1'} = 2.2 Hz, 1H, H₅), 5.23 (s, 1H, H_{1''}), 4.63 (dd, J_{H3''-H2''} = 6.3 Hz, J_{H3''-H4''} = 1.2 Hz, 1H, H_{3''}), 4.51 (d, J_{H2''-H3''} = 6.4 Hz, 1H, H_{2''}), 4.31–4.24 (m, 2 H, H_{5'}, H_{4''}), 4.16 (d, J_{H2'-H3'} = 3.9 Hz, 1H, H_{2'}), 4.17 (q, J_{H3***-H4***} = 7.1 Hz, 1H, H_{3***}), 4.09 (dd, J_{H4'-H3'} = 4.9 Hz, J_{H4'-H5'} = 1.4 Hz, 1H, H_{4'}), 4.01 (t, J_{H3'-H4'} = 4.6 Hz, 1H, H_{3'}), 3.52 (dd, J_{H5''a-H5''b} = 13 Hz, J_{H5''a-H6'} = 4.9 Hz, 1H, H_{5''a}), 3.43 (dd, J_{H5''b-H5''a} = 13 Hz, J_{H5''b-H4''} = 5.8 Hz, 1H, H_{5''b}), 3.40 (dd, J_{H6''a-H6''b} = 15.4 Hz, J_{H6''a-H5'} = 5.5 Hz, 1H, H_{6''a}), 3.21 (dd, J_{H6''b-H6''a} = 15.4 Hz, J_{H6''b-H5''} = 8.4 Hz, 1H, H_{6''b}), 2.12–2.00 (m, 4 H, H_{2*}, H_{2**}), 1.68 (q, J_{H7''a-H8''} = 7.4 Hz, 2 H, H_{7''a}), 1.55 (q, J_{H7''b-H8''} = 7.4 Hz, 2 H, H_{7''b}), 1.28–1.19 (m, 33 H, H_{3*-H10**}, H_{4*-H10*}, H_{4***}), 1.14–1.03 (m, 3H, H_{3*}), 0.91–0.83 (m, 30H, -SiC(CH₃)₃, H_{8''}, H_{11*}, H_{11**}), 0.09–0.07 (12 H, Si(CH₃)₂). ¹³C NMR (125 MHz, CDCl₃) δ 183.4 (C_{8'}), 166.8 (C_{7'}), 163.0 (C₄), 150.0 (C₂), 140.3 (C₆), 118.0 (C_{6''}), 112.3 (C_{1''}), 101.7 (C₅), 89.0 (C_{1'}), 86.1 (C_{2''}), 85.1 (C_{4''}), 84.7 (C_{4'}), 81.7 (C_{3''}), 78.3 (C_{5'}), 75.6 (C_{2'}), 71.8 (C_{3'}), 53.4 (C_{5''}), 38.5 (C_{1*}), 33.5 (C_{2*}), 33.4 (C_{2**}), 32.0, 29.7, 29.7, 29.5, 29.4, 29.3, 28.9 (C_{7''}), 27.3 (C_{7''}), 26.0 (SiC(CH₃)₃), 25.9 (SiC(CH₃)₃), 22.8 (C_{3*}), 18.0 (C_{3**}), 14.2 (C_{4***}, C_{11**}, C_{11*}), 8.5 (C_{8''}), 7.6 (C_{8''}), −4.0 (SiCH₃), −4.3(SiCH₃), −4.6(SiC), −4.7(SiC). HRMS ESI+ calcd. for C₅₅H₁₀₀N₇O₁₀Si₂⁺ (M + H)⁺ 1074.7064 found 1074.7060.

3.1.13. General Procedure for Compounds Deprotection

The deprotection of compounds **11a–11i** was performed according to reference [42] and afforded the fully deprotected compounds **12a–12i** in 22 to 85% yield over two steps.

3.1.14. Oxadiazole 12a

Compound **12a** was obtained from the protected oxadiazole **11a** (30 mg, 32 μmol, 1 equiv.) as a white solid (16.7 mg, 85% yield): R_f 0.15 (DCM/MeOH/NH₄OH 14% 80/18/2); [α]_D + 15 (c 1.0, CH₂Cl₂); IR (film): 2912, 2888, 2240, 1750, 1700, 1650, 1400, 1275, 1260, 1000,

764, 750.; ^1H NMR (500 MHz, MeOD) δ 7.80 (d, $J_{\text{H6-H5}} = 8.1\text{Hz}$, 1H, H₆), 5.77 (d, $J_{\text{H1}'\text{-H2}'}$ = 3.1Hz, 1H, H_{1'}), 5.73 (d, $J_{\text{H5-H6}} = 8.1\text{Hz}$, 1H, H₅), 5.14 (s, 1H, H_{1''}), 4.33–4.27 (m, 1H, H_{2'}), 4.18–4.12 (m, 2 H, H_{3'}, H_{4'}), 4.09 (t, $J_{\text{H4}''\text{-H5}''}$ = 7.1Hz, 1H, H_{4''}), 4.04 (m, 2 H, H_{2''}, H_{3''}), 3.98 (m, 1H, H_{5'}), 3.37–3.32 (m, 1H, H_{6'a}) 3.29–3.26 (m, 1H, H_{5'a}), 3.20 (dd, $J_{\text{H6}'\text{b-H6}'\text{a}} = 15.0$, $J_{\text{H6}'\text{b-H5}'}$ = 5.7 Hz, 1H, H_{6'b}), 3.11 (dd, $J_{\text{H5}''\text{b-H5}''\text{a}} = 13.0$, $J_{\text{H5}''\text{b-H4}''}$ = 7.1Hz, 1H, H_{5''b}), 2.91 (t, $J_{\text{H2}^*\text{-H3}^*}$ = 7.5 Hz, 2 H, H_{2*}), 1.79 (dt, $J_{\text{H3}^*\text{-H2}^*} = J_{\text{H3}^*\text{-H4}^*}$ = 7.4 Hz, 2 H, H_{3*}), 1.44–1.20 (m, 14 H), 0.89 (t, $J_{\text{H11}^*\text{-H10}^*}$ = 6.8 Hz, 3 H, H_{11*}).; ^{13}C NMR (125 MHz, MeOD) δ 181.9 (C_{1*}), 168.7 (C_{7'}), 166.1 (C₄), 152.1 (C₂), 142.2 (C₆), 111.0 (C_{1''}), 102.5 (C₅), 91.6 (C_{1'}), 85.7 (C_{3'}), 80.0 (C_{4''}), 78.1 (C_{5'}), 76.3 (C_{3''}), 75.5 (C_{2'}), 73.8 (C_{2''}), 71.3 (C_{4'}), 44.3 (C_{5''}), 33.0, 30.6 (C_{6'}), 30.39, 30.20, 30.02, 27.6 (C_{3*}), 27.1 (C_{2*}), 23.7, 14.4; HRMS ESI+ calcd. for C₂₇H₄₃N₅O₁₀ (M + H)⁺ 598.3083, found 598.3082.

3.1.15. Oxadiazole 12b

Compound **12b** was obtained from the protected oxadiazole **11b** (27 mg, 27 μmol , 1 equiv.) as a white solid (10.7 mg, 59% yield): R_f 0.15 (DCM/MeOH/NH₄OH 14% 80/18/2); $[\alpha]_D + 1$ (c 1.0, CH₃OH); IR (film): 2924, 2853, 1673, 1466, 1272, 1203, 1136, 800, 724; ^1H NMR (500 MHz, MeOD) δ 7.81 (d, $J_{\text{H6-H5}} = 8.1\text{Hz}$, 1H, H₆), 5.77 (d, $J_{\text{H1}'\text{-H2}'}$ = 3.2 Hz, 1H, H_{1'}), 5.72 (d, $J_{\text{H5-H6}} = 8.1\text{Hz}$, 1H, H₅), 5.14 (s, 1H, H_{1''}), 4.30 (td, $J_{\text{H5}'\text{-H6}'}$ = 6.5 Hz, $J_{\text{H5}'\text{-H4}'}$ = 2.5 Hz, 1H, H_{5'}), 4.19–4.01 (m, 5 H, H_{2'}, H_{3'}, H_{4'}, H_{3''}, H_{2''}), 3.98 (d, $J_{\text{H4}''\text{-H5}''}$ = 4.3 Hz, 1H, H_{4''}), 3.30–3.27 (m, 2 H, H_{6'ab}), 3.21 (dd, $J_{\text{H5}''\text{a-H4}''}$ = 14.9 Hz, $J_{\text{H5}''\text{a-H5}''\text{b}}$ = 5.7 Hz, 1H, H_{5''a}), 3.12 (dd, $J_{\text{H5}''\text{b-H4}''}$ = 13.0 Hz, $J_{\text{H5}''\text{b-H5}''\text{a}}$ = 9.0 Hz, 1H, H_{5''b}), 2.91 (t, $J_{\text{H1}^*\text{-H2}^*}$ = 7.5 Hz, 2H, H_{1*}), 1.82–1.76 (m, 2H, H_{2*}), 1.38–1.29 (m, 24 H, H_{3*-H14*}), 0.90 (t, $J_{\text{H15}^*\text{-H14}^*}$ = 7.0 Hz, 3H, H_{15*}).; ^{13}C NMR (125 MHz, MeOD) δ 181.1 (C_{8'}), 168.7 (C_{7'}), 166.1 (C₄), 152.0 (C₂), 142.2 (C₆), 110.9 (C_{1''}), 102.4 (C₅), 91.5 (C_{1'}), 85.6 (C_{2''}), 79.9 (C_{4'}), 78.0 (C_{5'}), 76.2 (C_{4''}), 75.5 (C_{2'}), 73.8 (C_{3''}), 71.2 (C_{3'}), 44.3 (C_{5''}), 33.0 (C_{6'}), 30.8, 30.7, 30.7, 30.5, 30.4, 30.3, 30.2, 30.0 (C_{4*-C14*}), 27.6 (C_{2*}), 27.1 (C_{1*}), 23.7 (C_{3*}), 14.4 (C_{15*}). HRMS ESI+ calcd. for C₃₂H₅₄N₅O₁₀⁺ (M + H)⁺ 668.3865 found 668.3860.

3.1.16. Oxadiazole 12c

Compound **12c** was obtained from the protected oxadiazole **11c** (28 mg, 27 μmol , 1 equiv.) as a colorless oil (9.2 mg, 40% yield): R_f 0.15 (DCM/MeOH/NH₄OH 14% 80/18/2); $[\alpha]_D + 0.8$ (c 1.0, CH₃OH); IR (film): 2921, 2851, 1672, 1432, 1275, 1204, 1138, 961, 800, 764.; ^1H NMR (500 MHz, MeOD) δ 7.81 (d, $J_{\text{H6-H5}} = 8.0\text{ Hz}$, 1H, H₆), 5.76 (d, $J_{\text{H1}'\text{-H2}'}$ = 3.2 Hz, 1H, H_{1'}), 5.72 (d, $J_{\text{H5-H6}} = 8.0\text{ Hz}$, 1H, H₅), 5.14 (s, 1H, H_{1''}), 4.30 (td, $J_{\text{H5}'\text{-H6}'}$ = 6.5 Hz, $J_{\text{H5}'\text{-H4}'}$ = 2.5 Hz, 1H, H_{5'}), 4.17–4.01 (m, 5 H, H_{2'}, H_{3'}, H_{4'}, H_{3''}, H_{2''}), 3.98 (d, $J_{\text{H4}''\text{-H5}''}$ = 4.1Hz, 1H, H_{4''}), 3.30–3.25 (m, 2 H, H_{6'ab}), 3.21 (dd, $J_{\text{H5}''\text{a-H4}''}$ = 15.0 Hz, $J_{\text{H5}''\text{a-H5}''\text{b}}$ = 5.6 Hz, 1H, H_{5''a}), 3.12 (dd, $J_{\text{H5}''\text{b-H4}''}$ = 13.0 Hz, $J_{\text{H5}''\text{b-H5}''\text{a}}$ = 9.0 Hz, 1H, H_{5''b}), 2.91 (t, $J_{\text{H1}^*\text{-H2}^*}$ = 7.5 Hz, 2 H, H_{1*}), 1.80–1.76 (m, 2 H, H_{2*}), 1.36–1.29 (m, 30 H, H_{3*-H17*}), 0.90 (t, $J_{\text{H15}^*\text{-H14}^*}$ = 6.9 Hz, 3H, H_{18*}).; ^{13}C NMR (125 MHz, MeOD) δ 181.8 (C_{8'}), 168.7 (C_{7'}), 166.1 (C₄), 152.0 (C₂), 142.2 (C₆), 110.9 (C_{1''}), 102.4 (C₅), 91.6 (C_{1'}), 85.6 (C_{2''}), 79.9 (C_{4'}), 78.1 (C_{5'}), 76.2 (C_{4''}), 75.5 (C_{2'}), 73.8 (C_{3''}), 71.2 (C_{3'}), 44.3 (C_{5''}), 33.0 (C_{6'}), 30.8, 30.5, 30.4, 30.3, 30.2, 30.0 (C_{4*-C17*}), 27.6 (C_{2*}), 27.1 (C_{1*}), 23.7 (C_{3*}), 14.4 (C_{18*}).; HRMS ESI+ calcd. for C₃₅H₆₀N₅O₁₀⁺ (M + H)⁺ 710.4335 found 710.4325.

3.1.17. Oxadiazole 12d

Compound **12d** was obtained from the protected oxadiazole **11d** (22 mg, 21 μmol , 1 equiv.) as a colorless oil (12 mg, 66% yield): R_f 0.15 (DCM/MeOH/NH₄OH 14% 80/18/2); $[\alpha]_D + 0.9$ (c 1.0, CH₃OH); IR (film): 3007, 2920, 2850, 1670, 1435, 1275, 1204, 1138, 960, 801, 764, 750; ^1H NMR (500 MHz, MeOD) δ 7.81 (d, $J_{\text{H6-H5}} = 8.1\text{Hz}$, 1H, H₆), 5.76 (d, $J_{\text{H1}'\text{-H2}'}$ = 3.3 Hz, 1H, H_{1'}), 5.73 (d, $J_{\text{H5-H6}} = 8.1\text{Hz}$, 1H, H₅), 5.34 (t, $J_{\text{H8}^*\text{-H9}^*}$ = 4.6 Hz, 2 H, H_{8*}, H_{9*}), 5.14 (s, 1H, H_{1''}), 4.30 (td, $J_{\text{H5}'\text{-H6}'}$ = 6.5 Hz, $J_{\text{H5}'\text{-H4}'}$ = 2.5 Hz, 1H, H_{5'}), 4.15–4.01 (m, 5 H, H_{2'}, H_{3'}, H_{4'}, H_{3''}, H_{2''}), 3.98 (d, $J_{\text{H4}''\text{-H5}''}$ = 4.3 Hz, 1H, H_{4''}), 3.29–3.25 (m, 2 H, H_{6'ab}), 3.21 (dd, $J_{\text{H5}''\text{a-H4}''}$ = 14.6 Hz, $J_{\text{H5}''\text{a-H5}''\text{b}}$ = 5.8 Hz, 1H, H_{5''a}), 3.12 (dd, $J_{\text{H5}''\text{b-H4}''}$ = 12.3 Hz, $J_{\text{H5}''\text{b-H5}''\text{a}}$ = 9.2 Hz, 1H, H_{5''b}), 2.91 (t, $J_{\text{H1}^*\text{-H2}^*}$ = 7.3 Hz, 2 H, H_{1*}), 2.06–2.01 (m, 4 H, H_{7*}, H_{10*}), 1.81–1.76

(m, 2 H, H₂*), 1.35–1.29 (m, 20 H, H₃*-H₆*, H₁₁*-H₁₆*), 0.91 (t, $J_{H_{15}^*-H_{14}^*} = 6.7$ Hz, 3H, H₁₇*); ¹³C NMR (125 MHz, MeOD) δ 181.8 (C₈'), 168.7 (C₇'), 166.1 (C₄), 152.0 (C₂), 142.2 (C₆), 130.9 (C₈*), 130.7 (C₉*), 110.9 (C₁''), 102.3 (C₅), 91.6 (C₁'), 85.5 (C₂''), 80.0 (C₄'), 78.1 (C₅''), 76.2 (C₄''), 75.5 (C₂''), 73.8 (C₃''), 71.2 (C₃'), 44.3 (C₅''), 33.0 (C₆'), 30.8, 30.7, 30.6, 30.4, 30.3, 30.3, 30.1, 30.0 (C₄*-C₆*, C₁₁*-C₁₆*), 28.1 (C₇*), 28.0 (C₁₀*), 27.6 (C₂*), 27.1 (C₁*), 23.7 (C₃*), 14.4 (C₁₇*). HRMS ESI– calcd. for C₃₄H₅₄N₅O₁₀[−] (M + H)[−] 692.3876 found 692.3890.

3.1.18. Oxadiazole 12e

Compound **12e** was obtained from the protected oxadiazole **11e** (20 mg, 21 μmol, 1 equiv.) as a colorless oil (8 mg, 60% yield): *R_f* 0.15 (DCM/MeOH/NH₄OH 14% 80/18/2); [α]_D + 1 (c 1.0, CH₃OH); IR (film): 3058, 2912, 2840, 1658, 1435, 1275, 1244, 1198, 993, 799, 751; ¹H NMR (500 MHz, MeOD) δ 8.10 (d, $J_{H_a-H_b} = 8.8$ Hz, 2 H, H_a), 7.81 (d, $J_{H_6-H_5} = 8.4$ Hz, 1H, H₆), 7.45 (t, $J_{H_d-H_e} = 8.0$ Hz, 2H, H_d), 7.25 (t, $J_{H_e-H_d} = 7.5$ Hz, 1H, H_e), 7.13–7.10 (m, 4 H, H_c, H_b), 5.78 (d, $J_{H_{1'}-H_{2'}} = 3.0$ Hz, 1H, H₁''), 5.70 (d, $J_{H_5-H_6} = 8.4$ Hz, 1H, H₅), 5.18 (s, 1H, H₁''), 4.38 (td, $J_{H_{5'}-H_{6'}} = 5.7$ Hz, $J_{H_{5'}-H_{4'}} = 3.1$ Hz, 1H, H₅''), 4.17–4.14 (m, 2 H, H₂'', H₃''), 4.09–4.05 (m, 3 H, H₄'', H₃'', H₂''), 3.99 (d, $J_{H_{4''}-H_{5''}} = 3.5$ Hz, 1H, H₄''), 3.38–3.32 (m, 2H, H_{6'}ab), 3.29–3.27 (m, $J_{H_{5''a}-H_{5''b}} = 5.8$ Hz, 1H, H₅''), 3.17–3.11 (m, 1H, H₅''); ¹³C NMR (125 MHz, MeOD) δ 176.6 (C₈''), 169.5 (C₇''), 166.0 (C₄), 163.6 (C₉*), 156.6 (C₁₀*), 152.1 (C₂), 142.2 (C₆), 131.3 (C_d), 131.2 (C_a), 126.0 (C_e), 121.3 (C_c), 119.0 (C_b), 110.8 (C₁''), 102.4 (C₅), 91.5 (C₁''), 85.7 (C₂''), 79.9 (C₄''), 78.0 (C₅''), 76.2 (C₄''), 75.4 (C₂''), 73.9 (C₃''), 71.3 (C₃'), 44.4 (C₅''), 30.4 (C₁₁*); HRMS ESI+ calcd. for C₂₉H₃₂N₅O₁₁⁺ (M + H)⁺ 626.2092 found 626.2078.

3.1.19. Oxadiazole 12f

Compound **12f** was obtained from the protected oxadiazole **11f** (44 mg, 41 μmol, 1 equiv.) as a colorless oil (22.8 mg, 63% yield): *R_f* 0.15 (DCM/MeOH/NH₄OH 14% 80/18/2); [α]_D + 8 (c 1.0, CH₃OH); IR (film): 3052, 2926, 2854, 1698, 1410, 1275, 1203, 1132, 965, 799, 764, 750; ¹H NMR (500 MHz, MeOD) δ 7.81 (d, $J_{H_6-H_5} = 8.1$ Hz, 1H, H₆), 5.77 (d, $J_{H_{1'}-H_{2'}} = 3.2$ Hz, 1H, H₁''), 5.73 (d, $J_{H_5-H_6} = 8.1$ Hz, 1H, H₅), 5.41–5.36 (m, 2 H, H₈'', H₉''), 5.14 (s, 1H, H₁''), 4.30 (td, $J_{H_{5'}-H_{6'}} = 6.5$ Hz, $J_{H_{5'}-H_{4'}} = 2.5$ Hz, 1H, H₅''), 4.16–4.02 (m, 5 H, H₂'', H₃'', H₄'', H₃'', H₂''), 3.98 (d, $J_{H_{4''}-H_{5''}} = 4.8$ Hz, 1H, H₄''), 3.30–3.25 (m, 2 H, H_{6'}ab), 3.21 (dd, $J_{H_{5''a}-H_{4''}} = 14.9$ Hz, $J_{H_{5''a}-H_{5''b}} = 5.7$ Hz, 1H, H₅''), 3.12 (dd, $J_{H_{5''b}-H_{4''}} = 13.1$ Hz, $J_{H_{5''b}-H_{5''a}} = 9.0$ Hz, 1H, H₅''), 2.91 (t, $J_{H_{11}^*-H_{2}^*} = 7.6$ Hz, 2H, H₁*), 2.00–1.95 (m, 4H, H₇*, H₁₀*), 1.81–1.76 (m, 2H, H₂*), 1.37–1.29 (m, 20H, H₃*-H₆*, H₁₁*-H₁₆*), 0.90 (t, $J_{H_{15}^*-H_{14}^*} = 6.9$ Hz, 3H, H₁₇*); ¹³C NMR (125 MHz, MeOD) δ 181.8 (C₈''), 168.7 (C₇''), 166.1 (C₄), 152.1 (C₂), 142.2 (C₆), 131.6 (C₈*), 131.4 (C₉*), 110.9 (C₁''), 102.4 (C₅), 91.5 (C₁'), 85.6 (C₂''), 80.0 (C₄'), 78.0 (C₅''), 76.2 (C₄''), 75.5 (C₂''), 73.8 (C₃''), 71.3 (C₃'), 44.3 (C₅''), 33.6 (C₇*), 33.5 (C₁₀*), 33.0 (C₆'), 30.7, 30.6, 30.5, 30.4, 30.3, 30.2, 30.0, 29.9 (C₄*-C₆*, C₁₁*-C₁₆*), 27.6 (C₂*), 27.1 (C₁*), 23.7 (C₃*), 14.4 (C₁₇*); HRMS ESI+ calcd. for C₃₄H₅₆N₅O₁₀⁺ (M + H)⁺ 694.4022 found 694.4012.

3.1.20. Oxadiazole 12g

Compound **12g** was obtained from the protected oxadiazole **11g** (20 mg, 20 μmol, 1 equiv.) as a colorless oil (12 mg, 63% yield): *R_f* 0.15 (DCM/MeOH/NH₄OH 14% 80/18/2); [α]_D + 1 (c 1.0, CH₃OH); IR (film): 3028, 2913, 2841, 1660, 1435, 1275, 1133, 993, 800, 764, 750; ¹H NMR (500 MHz, MeOD) δ 7.81 (d, $J_{H_6-H_5} = 8.3$ Hz, 1H, H₆), 7.23 (d, $J_{H_a-H_b} = 7.1$ Hz, 2 H, H_a), 7.16–7.11 (m, 3 H, H_b, H_c), 5.76 (d, $J_{H_{1'}-H_{2'}} = 3.1$ Hz, 1H, H₁''), 5.72 (d, $J_{H_5-H_6} = 8.2$ Hz, 1H, H₅), 5.14 (s, 1H, H₁''), 4.29 (td, $J_{H_{5'}-H_{6'}} = 6.5$ Hz, $J_{H_{5'}-H_{4'}} = 2.7$ Hz, 1H, H₅''), 4.15–4.01 (m, 5 H, H₂'', H₃'', H₄'', H₃'', H₂''), 3.98 (d, $J_{H_{4''}-H_{5''}} = 3.9$ Hz, 1H, H₄''), 3.30–3.26 (m, 2H, H_{6'}ab), 3.20 (dd, $J_{H_{5''a}-H_{4''}} = 15.3$ Hz, $J_{H_{5''a}-H_{5''b}} = 5.3$ Hz, 1H, H₅''), 3.11 (dd, $J_{H_{5''b}-H_{4''}} = 13.1$ Hz, $J_{H_{5''b}-H_{5''a}} = 9.0$ Hz, 1H, H₅''), 2.90 (t, $J_{H_{11}^*-H_{2}^*} = 7.4$ Hz, 2 H, H₁*), 2.59 (t, $J_{H_9^*-H_{10}^*} = 7.7$ Hz, 2 H, H₉*), 1.80–1.74 (m, 2 H, H₂*), 1.63–1.57 (m, 2 H, H₈*), 1.37–1.28 (m, 10 H, H₃*-H₇*); ¹³C NMR (125 MHz, MeOD) δ 181.8 (C₈''), 168.7 (C₇''), 166.1 (C₄), 152.1 (C₂), 143.9 (C₁₀*), 142.2 (C₆), 129.4 (C_a), 129.2 (C_b), 126.6 (C_c), 110.9 (C₁''), 102.4 (C₅), 91.5 (C₁'), 85.6 (C₂''), 79.9 (C₄''), 78.1 (C₅''), 76.2 (C₄''), 75.5 (C₂''), 73.8 (C₃''), 71.2 (C₃'), 44.3 (C₅''), 36.9 (C₉*), 32.7

(C_{6'}), 30.5, 30.4, 30.3, 30.2, 30.1, 29.9 (C_{3*}-C_{8*}), 27.6 (C_{2*}), 27.1 (C_{1*}); HRMS ESI+ calcd. for C₃₂H₄₆N₅O₁₀⁺ (M + H)⁺ 660.3239 found 660.3226.

3.1.21. Oxadiazole 12h

Compound **12h** was obtained from the protected oxadiazole **11h** (42 mg, 42 μmol, 1 equiv.) as a white solid (19 mg, 68% yield) and as a 1/1 mixture of stereoisomers: R_f 0.15 (DCM/MeOH/NH₄OH 14% 80/18/2); [α]_D + 1.4 (c 1.0, CH₃OH); IR (film): 2925, 2855, 1688, 1579, 1464, 1274, 1126, 748; ¹H NMR (500 MHz, MeOD) δ 7.80 (d, J_{H5-H6} = 8.1 Hz, 0.5H, H₆), 7.79 (d, J_{H5-H6} = 8.1 Hz, 0.5H, H₆), 5.75 (d, J_{H1'-H2'} = 3.1 Hz, 1H, H_{1'}), 5.72 (d, J_{H5-H6} = 8.1 Hz, 1H, H₅), 5.14 (s, 0.5H, H_{1''}), 5.12 (s, 0.5H, H_{1''}), 4.31 (td, J_{H5'-H6'a} = J_{H5'-H6'b} = 6.0, J_{H4'-H5'} = 3.0 Hz, 1H, H_{5'}), 4.26–4.16 (m, 2H, H_{3**}), 4.16–4.09 (m, 2H, H_{1*}, H_{2'}), 4.09–4.01 (m, 3H, H_{4''}, H_{4'}, H_{3''}), 3.97 (d, J_{H2''-H3''} = 3.5 Hz, 1H, H_{2''}), 3.38–3.32 (m, 1H, H_{6'a}), 3.30–3.26 (m, 1H, H_{5'a}), 3.23 (dd, J_{H6'a-H6'b} = 15.0, J_{H5'-H6'b} = 6.0 Hz, 1H, H_{6'b}), 3.14 (dd, J_{H5'a-H5'b} = 13.0, J_{H4''-H5'b} = 8.2 Hz, 1H, H_{5'b}), 2.17–1.95 (m, 2H, H_{2*}), 1.43–1.27 (m, 14H, H_{3*-H9*}), 1.25 (t, J_{H3*-H4**} = 7.1 Hz, 3H, H_{4**}), 0.90 (t, J_{H9*-H10*} = 6.9 Hz, 3H, H_{10*}); ¹³C NMR (125 MHz, MeOD) δ 178.28, 178.22 (C_{2**}), 170.5, 170.4 (C_{8'}), 169.22, 169.18 (C_{7'}), 166.16 (C₄), 152.1 (C₂), 142.2 (C₆), 111.1, 111.0 (C_{1''}), 102.4 (C₅), 91.60, 91.57 (C_{1'}), 85.9 (C_{4'}), 80.0 (C_{4''}), 78.3, 78.1 (C_{5'}), 76.3 (C_{2''}), 75.5 (C_{1*}), 73.9 (C_{3'}), 71.34, 71.30 (C_{2'}), 63.2 (C_{3**}), 44.3 (C_{5''}), 33.1, 31.2, 31.0, 30.6, 30.5, 30.2, 28.1, 23.7 (C_{2*-C9*}), 30.4 (C_{6'}), 14.5, 14.4 (C_{4**}, C_{10*}); HRMS ESI+ calcd. for C₃₀H₄₈N₅O₁₂⁺ (M + H)⁺ 670.3294 found 670.3320.

3.1.22. Oxadiazole 12i

Compound **12i** was obtained from the protected oxadiazole **11i** (34 mg, 32 μmol, 1 equiv.) as a colorless oil (5.3 mg, 22% yield): R_f 0.15 (DCM/MeOH/NH₄OH 14% 80/18/2); [α]_D + 1 (c 1.0, CH₃OH); IR (film): 2923, 1690, 1275, 1260, 764, 750; ¹H NMR (500 MHz, MeOD) δ 7.89 (d, J_{H6-H5} = 8.1 Hz, 1H, H₆), 5.81 (d, J_{H1'-H2'} = 2.7 Hz, 1H, H_{1'}), 5.74 (d, J_{H5-H6} = 8.1 Hz, 1H, H₅), 5.03 (s, 1H, H_{1''}), 4.30 (td, J_{H5'-H6'} = 6.3 Hz, J_{H5'-H4'} = 2.2 Hz, 1H, H_{5'}), 4.14–4.11 (m, 2H, H_{2'}, H_{3'}), 4.07–4.04 (m, 1H, H_{4'}), 3.98 (dd, J_{H3''-H2''} = 6.6 Hz, J_{H3''-H4''} = 4.8 Hz, 1H, H_{3''}), 3.93 (dd, J_{H2''-H3''} = 4.6 Hz, J_{H2''-H1''} = 1.2 Hz, 1H, H_{2''}), 3.88 (td, J_{H4''-H5''} = 7.1 Hz, J_{H4''-H3''} = 3.5 Hz, 1H, H_{4''}), 3.24 (dd, J_{H6'a-H5'} = 8.7 Hz, J_{H6'a-H6'b} = 6.3 Hz, 1H, H_{6'a}), 3.19 (dd, J_{H6'b-H5'} = 8.7 Hz, J_{H6'b-H5'} = 6.3 Hz, 1H, H_{6'b}), 3.06–3.00 (m, 1H, H_{1*}), 2.91 (dd, J_{H5'a-H4''} = 13.3 Hz, J_{H5'a-H5'b} = 3.7 Hz, 1H, H_{5'a}), 2.79 (dd, J_{H5'b-H4''} = 13.3 Hz, J_{H5'b-H5'a} = 7.5 Hz, 1H, H_{5'b}), 1.79–1.69 (m, 4H, H_{2*,H2**}), 1.35–1.17 (m, 34H, H_{3*-H10**}, H_{3*-H10*}), 0.91–0.88 (6H, H_{11*}, H_{11**}); ¹³C NMR (125 MHz, MeOD) δ 184.5 (C_{8'}), 168.6 (C_{7'}), 166.2 (C₄), 152.2 (C₂), 142.0 (C₆), 111.1 (C_{1''}), 102.4 (C₅), 91.0 (C_{1'}), 86.3 (C_{4'}), 84.5 (C_{4''}), 78.5 (C_{5'}), 76.8 (C_{2''}), 75.8 (C_{2'}), 73.3 (C_{3''}), 71.3 (C_{3'}), 45.3 (C_{5''}), 39.6 (C_{1*}), 34.6 (C_{2*}), 34.5 (C_{2**}), 33.0 (C_{9*}, C_{9**}), 30.8, 30.7, 30.4, 30.4 (C_{4*-C9*}, C_{4**}-C_{8**}), 28.2 (C_{3*}, C_{3**}), 23.7 (C_{10*}, C_{10**}), 14.4 (C_{11*}, C_{11**}); HRMS ESI+ calcd. for C₃₈H₆₆N₅O₁₀⁺ (M + H)⁺ 752.4804 found 752.4804.

3.1.23. Oxadiazole 12j

To a solution of oxadiazole **12h** (2.5 mg, 3.7 μmol, 1 equiv.) in methanol (0.4 mL) at 0 °C was added a solution of NH₄HCO₃ in water (0.1 M, 0.5 mL) and trimethylamine (14 μL, 99 μmol, 27 equiv.). After 48 h at 0 °C, the reaction mixture was diluted in 5 mL water, and the solution was freeze-dried. The residue was purified on a reverse phase column (Sep-Pak Cartridges C18) using a mixture of an aqueous solution NH₄HCO₃ (0.1 M) and acetonitrile (1/0 to 1/1, v/v). The fractions containing the product were freeze-dried to afford product **12j** as a white powder (0.4 mg) and as a 1/1 mixture of stereoisomers in 17% yield: R_f 0.07 (DCM/MeOH/NH₄OH 14% 80/18/2); ¹H NMR (500 MHz, MeOD) δ 7.87 (d, J_{H5-H6} = 8.1 Hz, 0.5H, H₆), 7.85 (d, J_{H5-H6} = 8.1 Hz, 0.5H, H₆), 5.80 (d, J_{H1'-H2'} = 3.4 Hz, 0.5H, H_{1'}), 5.79 (d, J_{H1'-H2'} = 3.4 Hz, 0.5H, H_{1'}), 5.74 (d, J_{H5-H6} = 8.1 Hz, 0.5H, H₅), 5.74 (d, J_{H5-H6} = 8.1 Hz, 0.5H, H₅), 5.12 (s, 0.5H, H_{1''}), 5.09 (s, 0.5H, H_{1''}), 4.37–4.31 (m, 1H, H_{5'}), 4.18–3.85 (m, 6H, H_{1*}, H_{2'}, H_{4''}, H_{4'}, H_{3''}, H_{2''}), 3.14–2.72 (m, 4H, H_{6'a}, H_{5'a}, H_{6'b}, H_{5'b}), 2.18–1.98 (m, 2H, H_{2*}), 1.40–1.22 (m, 14H, H_{3*-H9*}), 0.90 (t, J_{H9*-H10*} = 6.9 Hz, 3H, H_{10*}); ¹³C NMR (125 MHz, MeOD) δ 181.4 (C_{2**}), 170.3 (C_{8'}), 169.0 (C_{7'}), 166.3 (C₄), 152.3, 152.2 (C₂),

142.4, 142.2 (C₆), 110.4, 110.0 (C_{1''}), 102.57, 102.51 (C₅), 91.7 (C_{1'}), 86.4 (C_{4'}), 80.0 (C_{4''}), 78.1 (C_{5'}), 76.5 (C_{2''}), 75.55, 75.49 (C_{1*}), 73.7, 73.6 (C_{3'}), 71.4, 71.3 (C_{2'}), 44.94, 44.87 (C_{5''}), 33.1, 32.1, 31.9, 30.8, 30.7, 30.6, 30.5, 26.9, 23.7 (C_{2*}-C_{9*}, C_{6'}), 14.5 (C_{10*}); HRMS ESI+ calcd. for C₂₈H₄₄N₅O₁₂⁺ (M + H)⁺ 642.2942 found 642.2979.

3.2. Enzyme Assays

The inhibitory activity of the synthesized compounds 1–5 was determined as described in reference [41,42] except that compounds were tested at a final concentration of *m*. The compounds were evaluated on His-tagged *MraY* transferase purified from *Aquifex aeolicus* (*MraY*_{AA}) prepared as previously described by Chung et al. [37]. The assays were performed as previously described by Stachyra et al. [53].

3.3. Antibacterial Activity

Antibacterial activity was determined as previously described [41,42], but molecules were solubilized in 100% DMSO (cell culture grade) at 1 mg/mL concentration and 10-fold diluted in MHB just before utilization. The MHB-diluted solutions were then serially diluted in 5% DMSO-MHB, at final concentrations ranging from 50 mg/mL to 0.005 mg/mL for compounds and 6.25 to 5% for DMSO. Growth controls for strains indicated that DMSO does not inhibit growth at the highest concentration used in the test.

3.4. Docking

Docking experiments were performed according to the protocol previously described [41,42].

4. Conclusions

We report the synthesis of new inhibitors of the bacterial *MraY*_{AA} transferase displaying an aminoribosyl uridine scaffold substituted in 5' position by an oxadiazole linker bearing various hydrophobic substituents. Their straightforward synthesis relies on the microwave-assisted *O*-acylation of an amidoxime by various acyl chlorides followed by cyclization into the oxadiazole. Their biological activity was evaluated in vitro on purified *MraY*_{AA} and compared to that of a reference compound with a *N*-triazole as another heterocyclic linker. Nine out of the ten synthesized compounds revealed *MraY* inhibition with IC₅₀ ranging from 0.77 to 27.48 μM, the most active compound with a C₁₀ alkyl chain being slightly more active than the *N*-triazole reference compound. The binding mode of the inhibitors has been studied by docking experiments. The in cellulo evaluation of the synthesized inhibitors on different Gram-positive and Gram-negative bacterial strains only led to the poor activity of the two compounds on Gram-positive bacteria, showing that the further optimization of the lipophilic side chain is still required to improve the antibacterial activity.

Supplementary Materials: The following supporting information can be downloaded at: <https://www.mdpi.com/article/10.3390/antibiotics11091189/s1>, ¹H and ¹³C spectra of all compounds. Table S1: Antibacterial activity of compounds 12a–12i and reference compounds.

Author Contributions: Conceptualization, H.W., R.B.O., L.L.C., S.C.-V., M.B. and C.G.-P.; data curation, H.W., R.B.O., L.L.C., M.P., S.C.-V., M.B. and C.G.-P.; methodology, H.W., R.B.O., L.L.C., M.P., A.A., B.J., S.C.-V., M.B. and C.G.-P.; investigation, H.W., R.B.O., L.L.C., M.P., M.O., T.T., R.A., M.B. and A.A.; writing—original draft preparation, H.W., R.B.O., L.L.C., A.A., S.C.-V., M.B. and C.G.-P.; writing—review and editing, H.W., R.B.O., L.L.C., A.A., B.J., S.C.-V., M.B. and C.G.-P.; supervision, S.C.-V., M.B. and C.G.-P.; project administration, C.G.-P. All authors have read and agreed to the published version of the manuscript.

Funding: This research was supported by the “Centre National de la Recherche Scientifique” and the “Ministère de l’Enseignement Supérieur et de la Recherche”. H. W. thanks the Chinese Scholarship Council for the financial support of her PhD (201909505005).

Institutional Review Board Statement: Not applicable.

Informed Consent Statement: Not applicable.

Data Availability Statement: The data presented in this study are available in Supplementary Material.

Acknowledgments: We warmly thank Ahmed Bouhss (Université Paris-Saclay, INSERM U1204, Univ Evry) and D. Padovani (Université Paris Cité, CNRS) for their interest in this work and for helpful discussions. The assistance of P. Gerardo (Université Paris Cité) for low-resolution and high-resolution mass spectra analyses is gratefully acknowledged. We acknowledge the Macromolecular Modelling Platform and the NMR platform core facilities of the BioTechMed facilities INSERM US36 | CNRS UMS2009 | Université Paris Cité for docking and MD simulation and NMR experiments, respectively. H. W. thanks the Chinese Scholarship Council (201909505005) for the financial support of her PhD thesis.

Conflicts of Interest: The authors declare no conflict of interest.

References

1. Sherry, N.; Howden, B. Emerging Gram negative resistance to last-line antimicrobial agents fosfomycin, colistin and ceftazidime-avibactam—Epidemiology, laboratory detection and treatment implications. *Expert Rev. Anti Infect. Ther.* **2018**, *16*, 289–306. [[CrossRef](#)] [[PubMed](#)]
2. Jackson, N.; Czaplowski, L.; Piddock, L.J.V. Discovery and development of new antibacterial drugs: Learning from experience? *J. Antimicrob. Chemother.* **2018**, *73*, 1452–1459. [[CrossRef](#)]
3. Van Duijkeren, E.; Schink, A.K.; Roberts, M.C.; Wang, Y.; Schwarz, S. Mechanisms of bacterial resistance to antimicrobial agents. *Microbiol. Spectr.* **2018**, *6*. [[CrossRef](#)] [[PubMed](#)]
4. Murray, C.J.; Ikuta, K.S.; Sharara, F.; Swetschinski, L.; Aguilar, G.R.; Gray, A.; Han, C.; Bisignano, C.; Rao, P.; Wool, E.; et al. Global burden of bacterial antimicrobial resistance in 2019: A systematic analysis. *Lancet* **2022**, *399*, 629–655. [[CrossRef](#)]
5. Prestinaci, F.; Pezzotti, P.; Pantosti, A. Antimicrobial resistance: A global multifaceted phenomenon. *Pathog. Glob. Health* **2015**, *109*, 309–318. [[CrossRef](#)] [[PubMed](#)]
6. Wozniak, T.M.; Barnsbee, L.; Lee, X.J.; Pacella, R.E. Using the best available data to estimate the cost of antimicrobial resistance: A systematic review. *Antimicrob. Resist. Infect. Control* **2019**, *8*, 26. [[CrossRef](#)] [[PubMed](#)]
7. Xuemei, Z.; Lundborg, C.S.; Sun, X.; Hu, X.; Dong, H. Economic burden of antibiotic resistance in ESKAPE organisms: A systematic review. *Antimicrob. Resist. Infect. Control* **2019**, *8*, 137.
8. Innes, G.K.; Randad, P.R.; Korinek, A.; Davis, M.F.; Price, L.B.; So, A.D.; Heaney, C.D. External societal costs of antimicrobial resistance in humans attributable to antimicrobial use in livestock. *Annu. Rev. Public Health* **2020**, *41*, 141–157. [[CrossRef](#)]
9. Zhen, X.; Li, Y.; Chen, Y.; Dong, P.; Liu, S.; Dong, H. Effect of multiple drug resistance on total medical costs among patients with intra-abdominal infections in China. *PLoS ONE* **2018**, *13*, e0193977/1–e0193977/12. [[CrossRef](#)]
10. Barreteau, H.; Kovač, A.; Boniface, A.; Sova, M.; Gobec, S.; Blanot, D. Cytoplasmic steps of peptidoglycan biosynthesis. *FEMS Microbiol. Rev.* **2008**, *32*, 168–207. [[CrossRef](#)]
11. Bouhss, A.; Trunkfield, A.E.; Bugg, T.D.H.; Mengin-Lecreulx, D. The biosynthesis of peptidoglycan lipid-linked intermediates. *FEMS Microbiol. Rev.* **2008**, *32*, 208–233. [[CrossRef](#)]
12. Bugg, T.D.H.; Lloyd, A.J.; Roper, D.I. Phospho-MurNAc-pentapeptide translocase (MraY) as a target for antibacterial agents and antibacterial proteins. *Infect. Dis. Drug Targets* **2006**, *6*, 85–106. [[CrossRef](#)]
13. Bouhss, A.; Mengin-Lecreulx, D.; Le Beller, D.; van Heijenoort, J. Topological analysis of the MraY protein catalysing the first membrane step of peptidoglycan synthesis. *Mol. Microbiol.* **1999**, *34*, 576–585. [[CrossRef](#)]
14. Bouhss, A.; Crouvoisier, M.; Blanot, D.; Mengin-Lecreulx, D. Purification and characterization of the bacterial MraY translocase catalyzing the first membrane step of peptidoglycan biosynthesis. *J. Biol. Chem.* **2004**, *279*, 29974–29980. [[CrossRef](#)]
15. Al-Dabbagh, B.; Olatunji, S.; Crouvoisier, M.; El Ghachi, M.; Blanot, D.; Mengin-Lecreulx, D.; Bouhss, A. Catalytic mechanism of MraY and WeeA, two paralogues of the polyprenyl-phosphate N-acetylhexosamine 1-phosphate transferase superfamily. *Biochimie* **2016**, *127*, 249–257. [[CrossRef](#)]
16. Ubukata, M.; Isono, K.; Kimura, K.; Nelson, C.C.; McCloskey, J.A. The structure of liposidomycin B, an inhibitor of bacterial peptidoglycan synthesis. *J. Am. Chem. Soc.* **1998**, *110*, 4416–4417. [[CrossRef](#)]
17. Ubukata, M.; Isono, K.; Kimura, K.; Nelson, C.C.; Gregson, J.M.; McCloskey, J.A. Structure elucidation of liposidomyocins, a class of complex lipid nucleoside antibiotics. *J. Org. Chem.* **1992**, *57*, 6392–6403. [[CrossRef](#)]
18. Brandish, P.E.; Kimura, K.I.; Inukai, M.; Southgate, R.; Lonsdale, J.T.; Bugg, T.D.H. Modes of action of tunicamycin, liposidomycin B, and mureidomycin A: Inhibition of phospho-N-acetylmuramyl-pentapeptide translocase from Escherichia coli. *Antimicrob. Agents Chemother.* **1996**, *40*, 1640–1644. [[CrossRef](#)]
19. McDonald, L.A.; Barbieri, L.R.; Carter, G.T.; Lenoy, E.; Lotvin, J.; Petersen, P.J.; Siegel, M.M.; Singh, G.; Williamson, R.T. Structures of the Muraymycins, novel peptidoglycan biosynthesis inhibitors. *J. Am. Chem. Soc.* **2002**, *124*, 10260–10261. [[CrossRef](#)]
20. Igarashi, M.; Nakagawa, N.; Doi, S.; Hattori, N.; Naganawa, H.; Hamada, M. Caprazamycin B, a novel anti-tuberculosis antibiotic, from *Streptomyces* sp. *J. Antibiot.* **2003**, *56*, 580–583. [[CrossRef](#)]

21. Igarashi, M.; Takahashi, Y.; Shitara, T.; Nakamura, H.; Naganawa, H.; Miyake, T.; Akamatsu, Y. Caprazamycins, novel liponucleoside antibiotics, from *Streptomyces* sp. *J. Antibiot.* **2005**, *58*, 327–337. [[CrossRef](#)]
22. Dini, C.; Collette, P.; Drochon, N.; Guillot, J.C.; Lemoine, G.; Mauvais, P.; Aszodi, J. Synthesis of the nucleoside moiety of liposidomycins: Elucidation of the pharmacophore of this family of MraY inhibitors. *Bioorg. Med. Chem. Lett.* **2000**, *10*, 1839–1843. [[CrossRef](#)]
23. Dini, C.; Drochon, N.; Feteanu, S.; Guillot, J.C.; Peixoto, C.; Aszodi, J. Synthesis of analogues of the O-beta-D-ribofuranosyl nucleoside moiety of liposidomycins. Part 1: Contribution of the amino group and the uracil moiety upon the inhibition of MraY. *Bioorg. Med. Chem. Lett.* **2001**, *11*, 529–531. [[CrossRef](#)]
24. Dini, C.; Drochon, N.; Guillot, J.C.; Mauvais, P.; Walter, P.; Aszodi, J. Synthesis of analogues of the O-beta-D-ribofuranosyl nucleoside moiety of liposidomycins. Part 2: Role of the hydroxyl groups upon the inhibition of MraY. *Bioorg. Med. Chem. Lett.* **2001**, *11*, 533–536. [[CrossRef](#)]
25. Patel, B.; Ryan, P.; Makwana, V.; Zunk, M.; Rudrawar, S.; Grant, G. Caprazamycins: Promising lead structures acting on a novel antibacterial target MraY. *Eur. J. Med. Chem.* **2019**, *171*, 462–474. [[CrossRef](#)]
26. Fer, M.J.; Le Corre, L.; Pietrancosta, N.; Evrard-Todeschi, N.; Olatunji, S.; Bouhss, A.; Calvet-Vitale, S.; Gravier-Pelletier, C. Bacterial transferase MraY, a source of inspiration towards new antibiotics. *Curr. Med. Chem.* **2018**, *25*, 6013–6025. [[CrossRef](#)]
27. Wiegmann, D.; Koppermann, S.; Wirth, M.; Niro, G.; Leyerer, K.; Ducho, C. Muraymycin nucleoside-peptide antibiotics: Uridine-derived natural products as lead structures for the development of novel antibacterial agents. *Beilstein J. Org. Chem.* **2016**, *12*, 769–795. [[CrossRef](#)]
28. Ichikawa, S.; Yamaguchi, M.; Matsuda, A. Antibacterial nucleoside natural products inhibiting phospho-MurNAc-pentapeptide translocase; chemistry and structure-activity relationship. *Curr. Med. Chem.* **2015**, *22*, 3951–3979. [[CrossRef](#)]
29. Tanino, T.; Ichikawa, S.; Al-Dabbagh, B.; Bouhss, A.; Oyama, H.; Matsuda, A. Synthesis and biological evaluation of muraymycin analogues active against anti-drug-resistant bacteria. *ACS Med. Chem. Lett.* **2010**, *1*, 258–262. [[CrossRef](#)]
30. Ichikawa, S.; Yamaguchi, M.; Shang Hsuan, L.; Kato, Y.; Matsuda, A. Carbaprazamycins: Chemically stable analogues of the caprazamycin nucleoside antibiotics. *ACS Infect. Dis.* **2015**, *1*, 151–156. [[CrossRef](#)] [[PubMed](#)]
31. Wiegmann, D.; Koppermann, S.; Ducho, C. Aminoribosylated analogues of muraymycin nucleoside antibiotics. *Molecules* **2018**, *23*, 3085. [[CrossRef](#)] [[PubMed](#)]
32. Leyerer, K.; Koppermann, S.; Ducho, C. Solid phase-supported synthesis of muraymycin analogues. *Eur. J. Org. Chem.* **2019**, *45*, 7420–7431. [[CrossRef](#)]
33. Patel, B.; Kerr, R.V.; Malde, A.K.; Zunk, M.; Bugg, T.D.H.; Grant, G.; Rudrawar, S. Simplified novel Muraymycin analogues; using a serine template strategy for linking key pharmacophores. *ChemMedChem* **2020**, *15*, 1429–1438. [[CrossRef](#)] [[PubMed](#)]
34. Kwak, S.H.; Lim, W.Y.; Hao, A.; Mashalidis, E.H.; Kwon, D.Y.; Jeong, P.; Kim, M.J.; Lee, S.Y.; Hong, J. Synthesis and evaluation of cyclopentane-based muraymycin analogs targeting MraY. *Eur. J. Med. Chem.* **2021**, *215*, 113272. [[CrossRef](#)]
35. Okamoto, K.; Ishikawa, A.; Okawa, R.; Yamamoto, K.; Sato, T.; Yokota, S.-I.; Chiba, K.; Ichikawa, S. Design, synthesis and biological evaluation of simplified analogues of MraY inhibitory natural product with rigid scaffold. *Bioorg. Med. Chem.* **2022**, *55*, 116556. [[CrossRef](#)] [[PubMed](#)]
36. Kusaka, S.; Yamamoto, K.; Shinohara, M.; Minato, Y.; Ichikawa, S. Design, synthesis and conformation-activity relationship analysis of LNA/BNA-type 5-O-aminoribosyluridine as MraY inhibitors. *Bioorg. Med. Chem.* **2022**, *65*, 116744. [[CrossRef](#)]
37. Chung, B.C.; Mashalidis, E.H.; Tanino, T.; Kim, M.; Matsuda, A.; Hong, J.; Ichikawa, S.; Lee, S.Y. Structural insights into inhibition of lipid I production in bacterial cell wall synthesis. *Nature* **2016**, *533*, 557–560. [[CrossRef](#)]
38. Mashalidis, E.H.; Kaeser, B.; Terasawa, Y.; Katsuyama, A.; Kwon, D.Y.; Lee, K.; Hong, J.; Ichikawa, S.; Lee, S.Y. Chemical logic of MraY inhibition by antibacterial nucleoside natural products. *Nat. Commun.* **2019**, *10*, 2917–2928. [[CrossRef](#)]
39. Fer, M.J.; Olatunji, S.; Bouhss, A.; Calvet-Vitale, S.; Gravier-Pelletier, C. Toward analogues of MraY natural inhibitors: Synthesis of 5-triazole-substitute-aminoribosyl uridines through a Cu-catalyzed azide-alkyne cycloaddition. *J. Org. Chem.* **2013**, *78*, 10088–10105. [[CrossRef](#)]
40. Fer, M.J.; Bouhss, A.; Patrão, M.; Le Corre, L.; Pietrancosta, N.; Amoroso, A.; Joris, B.; Mengin-Lecreulx, D.; Calvet-Vitale, S.; Gravier-Pelletier, C. 5'-Methylene-triazole-substituted-aminoribosyl uridines as MraY inhibitors: Synthesis, biological evaluation and molecular modeling. *Org. Biomol. Chem.* **2015**, *13*, 7193–7222. [[CrossRef](#)]
41. Oliver, M.; Le Corre, L.; Poinot, M.; Corio, A.; Madegard, L.; Bosco, M.; Amoroso, A.; Joris, B.; Auger, R.; Touzé, T.; et al. Synthesis, biological evaluation and molecular modeling of urea-containing MraY inhibitors. *Org. Biomol. Chem.* **2021**, *19*, 5844–5866. [[CrossRef](#)] [[PubMed](#)]
42. Oliver, M.; Le Corre, L.; Poinot, M.; Bosco, M.; Wan, H.; Amoroso, A.; Joris, B.; Bouhss, A.; Calvet-Vitale, S.; Gravier-Pelletier, C. A sub-micromolar MraYAA Inhibitor with an aminoribosyl uridine structure and a (S,S)-tartaric diamide: Synthesis, biological evaluation and molecular modeling. *Molecules* **2022**, *27*, 1769. [[CrossRef](#)] [[PubMed](#)]
43. Hirano, S.; Ichikawa, S.; Matsuda, A. Total synthesis of caprazol, a core structure of the caprazamycin antituberculosis antibiotics. *Angew. Chem. Int. Ed.* **2005**, *44*, 1854–1856. [[CrossRef](#)]
44. Fer, M.J.; Doan, P.; Prangé, T.; Calvet-Vitale, S.; Gravier-Pelletier, C. A diastereoselective synthesis of 5'-substituted-uridine derivatives. *J. Org. Chem.* **2014**, *79*, 7758–7765. [[CrossRef](#)]
45. Paz, N.R.; Santana, A.G.; Francisco, C.G.; Suárez, E.; González, C.C. Synthesis of tetrazole-fused glycosides by a tandem fragmentation-cyclization reaction. *Org. Lett.* **2012**, *14*, 3388–3392. [[CrossRef](#)]

46. Dini, C.; Didier-Laurent, S.; Drochon, N.; Feteanu, S.; Guillot, J.C.; Monti, F.; Uridat, E.; Zhang, J.; Aszodi, J. Synthesis of sub-micromolar inhibitors of MraY by exploring the region originally occupied by the diazepanone ring in the liposidomycin structure. *Biorg. Med. Chem. Lett.* **2002**, *12*, 1209–1213. [[CrossRef](#)]
47. Kourra, C.; Klotter, F.; Sladojevich, F.; Dixon, D.J. Alkali base-initiated michael addition/alkyne carbocyclization cascades. *Org. Lett.* **2012**, *14*, 1016–1019. [[CrossRef](#)]
48. Wçlk, C.; Drescher, S.; Meister, A.; Blume, A.; Langner, A.; Dobner, B. General synthesis and physicochemical characterisation of a series of peptide-mimic lysine-based amino-functionalised lipids. *Chem. Eur. J.* **2013**, *19*, 12824–12838.
49. Santucci, P.; Dedaki, C.; Athanasoulis, A.; Gallorini, L.; Munoz, A.; Canaan, S.; Cavalier, J.F.; Magrioti, V. Synthesis of long-chain-lactones and their antibacterial activities against pathogenic Mycobacteria. *ChemMedChem* **2019**, *14*, 349–358. [[CrossRef](#)]
50. Ehsan, M.; Du, Y.; Scull, N.J.; Tikhonova, E.; Tarrasch, J.; Mortensen, J.S.; Loland, C.J.; Skiniotis, G.; Guan, L.; Byrne, B.; et al. Highly branched pentasaccharide-bearing amphiphiles for membrane protein studies. *J. Am. Chem. Soc.* **2016**, *138*, 3789–3796. [[CrossRef](#)]
51. Chung, B.C.; Zhao, J.; Gillespie, R.A.; Kwon, D.Y.; Guan, Z.; Hong, J.; Zhou, P.; Lee, S.Y. Crystal structure of MraY, an essential membrane enzyme for bacterial cell wall synthesis. *Science* **2013**, *341*, 1012–1016. [[CrossRef](#)]
52. Wu, G.S.; Robertson, D.H.; Brooks, C.L.; Vieth, M. Detailed analysis of grid-based molecular docking: A case study of CDOCKER-A CHARMM-based MD docking algorithm. *J. Comput. Chem.* **2003**, *24*, 1549–1562. [[CrossRef](#)]
53. Stachyra, T.; Dini, C.; Ferrari, P.; Bouhss, A.; van Heijenoort, J.; Mengin-Lecreulx, D.; Blanot, D.; Bitton, J.; Le Beller, D. Fluorescence detection-based functional assay for high-throughput screening for MraY. *Antimicrob. Agents Chemother.* **2004**, *48*, 897–902. [[CrossRef](#)]